COBE: A Radiological Analysis

Pierre-Marie Robitaille

Department of Radiology, The Ohio State University, 395 W. 12th Ave, Suite 302, Columbus, Ohio 43210, USA

E-mail: robitaille.1@osu.edu

The COBE Far Infrared Absolute Spectrophotometer (FIRAS) operated from ∼30 to ∼3,000 GHz (1–95 cm^{-1}) and monitored, from polar orbit (∼900 km), the ∼3 K microwave background. Data released from FIRAS has been met with nearly universal admiration. However, a thorough review of the literature reveals significant problems with this instrument. FIRAS was designed to function as a differential radiometer, wherein the sky signal could be nulled by the reference horn, Ical. The null point occurred at an Ical temperature of 2.759 K. This was 34 mK above the reported sky temperature, 2.725±0.001 K, a value where the null should ideally have formed. In addition, an 18 mK error existed between the thermometers in Ical, along with a drift in temperature of ∼3 mK. A 5 mK error could be attributed to Xcal; while a 4 mK error was found in the frequency scale. A direct treatment of all these systematic errors would lead to a ∼64 mK error bar in the microwave background temperature. The FIRAS team reported ∼1 mK, despite the presence of such systematic errors. But a 1 mK error does not properly reflect the experimental state of this spectrophotometer. In the end, all errors were essentially transferred into the calibration files, giving the appearance of better performance than actually obtained. The use of calibration procedures resulted in calculated Ical emissivities exceeding 1.3 at the higher frequencies, whereas an emissivity of 1 constitutes the theoretical limit. While data from 30–60 GHz was once presented, these critical points are later dropped, without appropriate discussion, presumably because they reflect too much microwave power. Data obtained while the Earth was directly illuminating the sky antenna, was also discarded. From 300–660 GHz, initial FIRAS data had systematically growing residuals as frequencies increased. This suggested that the signal was falling too quickly in the Wien region of the spectrum. In later data releases, the residual errors no longer displayed such trends, as the systematic variations had now been absorbed in the calibration files. The FIRAS team also cited insufficient bolometer sensitivity, primarily attributed to detector noise, from 600–3,000 GHz. The FIRAS optical transfer function demonstrates that the instrument was not optimally functional beyond 1,200 GHz. The FIRAS team did not adequately characterize the FIRAS horn. Established practical antenna techniques strongly suggest that such a device cannot operate correctly over the frequency range proposed. Insufficient measurements were conducted on the ground to document antenna gain and field patterns as a full function of frequency and thereby determine performance. The effects of signal diffraction into FIRAS, while considering the Sun/Earth/RF shield, were neither measured nor appropriately computed. Attempts to establish antenna side lobe performance in space, at 1,500 GHz, are well outside the frequency range of interest for the microwave background (<600 GHz). Neglecting to fully evaluate FIRAS prior to the mission, the FIRAS team attempts to do so, on the ground, in highly limited fashion, with a duplicate Xcal, nearly 10 years after launch. All of these findings indicate that the satellite was not sufficiently tested and could be detecting signals from our planet. Diffraction of earthly signals into the FIRAS horn could explain the spectral frequency dependence first observed by the FIRAS team: namely, too much signal in the Jeans-Rayleigh region and not enough in the Wien region. Despite popular belief to the contrary, COBE has not proven that the microwave background originates from the universe and represents the remnants of creation.

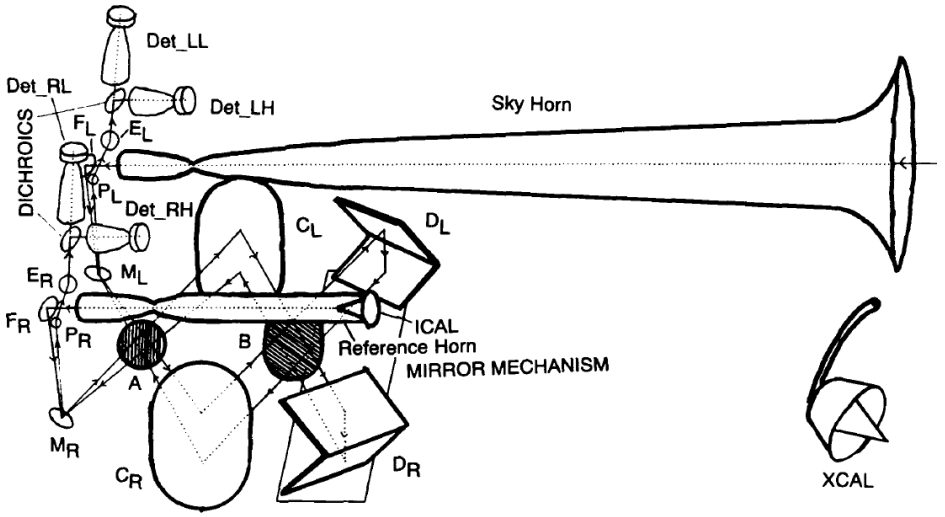

Fig. 1: Schematic representation of the COBE FIRAS instrument reproduced from [38]. The spectrometer is based on an interferometer design wherein the signal from the sky horn is being compared with that provided by the reference horn. Each of the input signals is split by grid polarizers, reflected by mirrors, and sent down the arms of the interferometer. Two output ports receive the resultant signal. An internal calibrator, Ical, equipped with two germanium resistance thermometers (GRT), provides signal to the reference horn. During calibration, the external calibrator, Xcal, is inserted into the sky horn. Xcal is monitored by three GRTs. The interferometer assembly includes a single mirror transport mechanism (MTM). Specific details can be found in [38]. No knowledge about the functioning of FIRAS, beyond that contained in this figure legend, is required to follow this work. The central elements are simply that FIRAS is made up of a sky horn, a reference horn, Ical (2 thermometers), and Xcal (3 thermometers). Reproduced by permission of the AAS.

1 Introduction

Conceding that the microwave background [1] must arise from the cosmos [2], scientists have dismissed the idea that the Earth itself could be responsible for this signal [3–7]. Most realize that the astrophysical claims are based on the laws of thermal emission [8–12]. Yet, few have ever personally delved into the basis of these laws [13–17]. At the same time, it is known that two satellites, namely COBE [18] and WMAP [19], support the cosmological interpretation [2]. As such, it seems impossible that an alternative explanation of the findings could ever prevail.

In late 2006, I prepared a detailed review of WMAP which uncovered many of the shortcomings of this instrument [20]. A range of issues were reported, including: 1) the inability to properly address the galactic foreground, 2) dynamic range issues, 3) a lack of signal to noise, 4) poor contrast, 5) yearly variability, and 6) unjustified changes in processing coefficients from year to year. In fact, WMAP brought only sparse information to the scientific community, related to the dipole and to point sources.

Nonetheless, the COBE satellite, launched in 1989, continues to stand without challenge in providing empirical proof that the microwave background did come from the universe. If COBE appears immune to criticism, it is simply because scientists outside the cosmological community have not taken the necessary steps to carefully analyze its results. Such an analysis of COBE, and specifically the Far Infrared Absolute Spectrophotometer, FIRAS, is provided in the pages which follow. Significant problems exist with FIRAS. If anything, this instrument provides tangential evidence for an earthly source, but the data was discounted. A brief discussion of the Differential Microwave Radiometers, DMR, outlines that the anisotropy maps, and the multipoles which describe them, are likely to represent a signal processing artifact.

1.1 The microwave background

When the results of the Cosmic Background Explorer (COBE) were first announced, Stephen Hawking stated that this "*was the scientific discovery of the century, if not of all time*" [21, book cover], [22, p. 236]. The Differential Microwave Radiometers (DMR) were said to have detected "*wrinkles in time*", the small anisotropies overlaid on the fabric of a nearly isotropic, or uniform, microwave background [21]. As for the COBE Far Infrared Absolute Spectrophotometer, FIRAS (see Figure 1), it had seemingly produced the most perfect blackbody spectrum ever recorded [23–45]. The blackbody curve deviated from ideality by less than 3.4×10^{-8} ergs cm^{-2} s^{-1} sr^{-1} cm [35] from $\sim$60–600 GHz. Eventually, the FIRAS team would publish that the "*rms deviations are less than 50 parts per million of the peak of the cosmic microwave background radiation*" [39]. As seen in Figure 2, the signal was so powerful that the error bars in its detection would form but a slight portion of the line used to draw the spectrum [39]. For its part, the Differential Microwave Radiometers (DMR), beyond the discovery of the anisotropies [21], had also confirmed the motion of the Earth through the

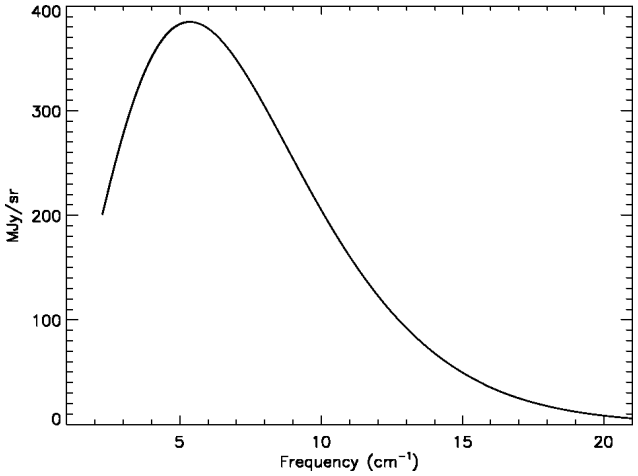

Fig. 2: Spectrum of the microwave background reproduced from [39]. This figure is well known for the claim that the error bars it contains are but a small fraction of the line width used to draw the spectrum. While this curve appears to represent a blackbody, it should be recalled that FIRAS is only sensitive to the difference between the sky and Xcal. This plot therefore reflects that the signal from the sky, after extensive calibration, is indistinguishable from that provided by Xcal. Since the latter is presumed to be a perfect blackbody, then such a spectrum is achieved for the sky. Note that the frequency axis is offset and all data below 2 cm^{-1} have been excluded. Reproduced by permission of the AAS.

local group, as established by a microwave dipole [46–49].

Over one thousand professional works have now appeared which directly utilize, or build upon, the COBE results [22, p. 247]. Yet, sparse concern can be found relative to any given aspect of the COBE project. Eventually, George Smoot and John Mather, the principle investigators for the DMR and FIRAS projects, would come to share the 2006 Nobel Prize in physics. Less than 30 years had elapsed since Arno Penzias and Robert Wilson received the same honor, in 1978, for the discovery of the $\sim$3 K microwave background [1].

Before the background was officially reported in the literature [1], the origin of the signal had already been advanced by Dicke et al. [2]. The interpretive paper [2] had immediately preceded the publication of the seminal discovery [1]. If the microwave background was thermal in origin [8–12], it implied a source at $\sim$3 K. Surely, such a signal could not come from the Earth. For the next 40 years, astrophysics would remain undaunted in the pursuit of the spectrum, thought to have stemmed from the dawn of creation. Smoot writes: "*Penzias and Wilson's discovery of the cosmic microwave background radiation was a fatal blow to the steady state theory*" [21, p. 86]. The steady state theory of the universe [50, 51] was almost immediately abandoned and astrophysics adopted Lemaître's concept of the primordial atom [52], later known as the Big Bang. Cosmologists advanced that mankind knew the average temperature of the entire universe. Thanks to COBE, cosmology was thought to have become a precision science [53, 54].

Throughout the detection history of the microwave background, it remained puzzling that the Earth itself never provided interference with the measurements. Water, after all, acts as a powerful absorber of microwave radiation. This is well understood, both at sea aboard submarines, and at home, within microwave ovens. As such, it seemed unlikely that the surface of our planet was microwave silent in every CMB experiment which preceded COBE. The only interference appeared to come from the atmosphere [55–57]. The latter was recognized as a powerful emitter of microwave radiation. The presence of water absorption/emission lines and of the water continuum, within the atmosphere, was well documented [55–57]. Nonetheless, emission from the Earth itself was overlooked.

The microwave signal is isotropic [1], while the Earth is anisotropic. The Earth experiences a broad range of real temperatures, which vary according to location and season. Yet, the background is found to be independent of seasonal variation [1]. The signal is definitely thermal in origin [9–17]. Most importantly, it is completely free from earthly contamination. The background appears to monitor a source temperature near $\sim$3 K. Earthly temperatures average $\sim$300 K and seldom fall below $\sim$200 K, even at the poles. It seems impossible that the Earth could constitute the source of this signal [3–7]. Everything can be reconsidered, only if the temperature associated with the microwave background signature is not real. Namely, that the source temperature is much higher than the temperature reported by the photons it emits. Insight in this regard can be gained by returning to the laws of thermal emission [8–12], as I have outlined [13–17].

1.2 Kirchhoff's law

One hundred and fifty years have now passed, since Kirchhoff first advanced the law upon which the validity of the microwave background temperature rests [9]. His law of thermal emission stated that radiation, at equilibrium with the walls of an enclosure, was always black, or normal [9, 10]. This was true in a manner independent of the nature of the enclosure. Kirchhoff's law was so powerful that it would become the foundation of contemporary astrophysics. By applying this formulation, the surface temperatures of all the stars could be evaluated, with the same ease as measuring the temperature of a brick-lined oven. Planck would later derive the functional form of blackbody radiation, the right-hand side of Kirchhoff's law, and thereby introduce the quantum of action [10]. However, since blackbody radiation only required enclosure and was independent of the nature of the walls, Planck did not link this process to a specific physical cause [13–17]. For astrophysics, this meant that any object could produce a blackbody spectrum. All that was required was mathematics and the invocation of thermal equilibrium. Even the requirement for enclosure was soon discarded. Processes occurring far out of equilibrium, such as the radiation of a star, and the alleged

expansion of the universe, were thought to be suitable candidates for the application of the laws of thermal emission [2]. To aggravate the situation, Kirchhoff had erred in his claim of universality [13–17]. In actuality, blackbody radiation was not universal. It was limited to an idealized case which, at the time, was best represented by graphite, soot, or carbon black [13–17]. Nothing on Earth has been able to generate the elusive blackbody over the entire frequency range and for all temperatures. Silver enclosures could never produce blackbody spectra. Kirchhoff's quest for universality was futile [13–17]. The correct application of the laws of thermal emission [8–12] requires the solid state. Applications of the laws to other states of matter, including liquids, gases, stars, and primordial atoms, constitute unjustified extensions of experimental realities and theoretical truths [13–17].

Since the source of the microwave background [1] could not possibly satisfy Kirchhoff's requirement for an enclosure [9], its $\sim$3 K temperature might only be apparent [13–17]. The temperature of the source could be very different than the temperature derived from its spectrum. Planck, indeed, advanced the same idea relative to using the laws of thermal emission to measure the surface temperature of the Sun. He wrote: "*Now the apparent temperature of the sun is obviously nothing but the temperature of the solar rays, depending entirely on the nature of the rays, and hence a property of the rays and not a property of the sun itself. Therefore it would be, not only more convenient, but also more correct, to apply this notation directly, instead of speaking of a fictitious temperature of the sun, which can be made to have a meaning only by the introduction of an assumption that does not hold in reality*" [58, §101]. Without a known enclosure, spectra appearing Planckian in nature do not necessarily have a direct link to the actual temperature of the source. The Sun operates far out of thermal equilibrium by every measure, as is evident by the powerful convection currents on its surface [59]. Furthermore, because it is not enclosed within a perfect absorber, its true surface temperature cannot be derived from the laws of thermal emission [59]. These facts may resemble the points to which Planck alludes.

1.3 The oceans of the Earth

The COBE team treats the Earth as a blackbody source of emission at $\sim$280 K [48]. Such a generalization seems plausible at first, particularly in the near infrared, as revealed by the remote sensing studies [60, 61]. However, FIRAS is making measurements in the microwave and far-infrared regions of the spectrum. It is precisely in this region that these assumptions fail. Furthermore, the FIRAS team is neglecting the fact that 70% of the planet is covered with water. Water is far from acting as a blackbody, either in the infrared or in the microwave. Using remote sensing, it has been well established that rainfall causes a pronounced drop in terrestrial brightness temperatures in a manner which is proportional to the rate of precipitation. In the microwave region, large bodies of water, like the oceans, display brightness temperatures which vary from a few Kelvin to $\sim$300 K, as a function of angle of observation, frequency, and polarization (see Figure 11.45 in [62]). Since the oceans are not enclosed, their thermal emission profiles do not necessarily correspond to their true temperatures. The oceans of the Earth, like the Sun, sustain powerful convection currents. Constantly striving for equilibrium, the oceans also fail to meet the requirements for being treated as a blackbody [13–17].

In order to understand how the oceans emit thermal radiation, it is important to consider the structure of water itself [6]. An individual water molecule is made up of two hydroxyl bonds, linking a lone oxygen atom with two adjacent hydrogens (H$-$O$-$H). These are rather strong bonds, with force constants of $\sim 8.45 \times 10^5$ dyn/cm [6]. In the gas phase, it is known that the hydroxyl bonds emit in the infrared region. The O$-$H stretch can thus be found near 3,700 cm^{-1}, while the bending mode occurs near 1,700 cm^{-1} [63]. In the condensed state, liquid water displays corresponding emission bands, near 3,400 cm^{-1} and 1,644 cm^{-1} [63, p. 220]. The most notable change is that the O$-$H stretching mode is displaced to lower frequencies [63]. This happens because water molecules, in the condensed state (liquid or solid), can interact weakly with one another, forming hydrogen bonds [63]. The force constant for the hydrogen bond ($H_2O \cdots HOH$) has been determined in the water dimer to be on the order of $\sim 0.108 \times 10^5$ dyn/cm [6, 64, 65]. But, in the condensed state, a study of rearrangement energetics points to an even lower value for the hydrogen bond force constant [66]. In any event, water, through the action of the hydrogen bond, should be emitting in the microwave and far-IR regions [6, 63]. Yet, this emission has never been detected. Perhaps, the oceanic emission from hydrogen bonds has just been mistaken for a cosmic source [2].

1.4 Ever-present water

1.4.1 Ground-based measurements

From the days of Penzias and Wilson [1], ground-based measurements of the microwave background have involved a correction for atmospheric water contributions (see [56] for an in-depth review). By measuring the emission of the sky at several angles (at least two), a correction for atmospheric components was possible. Further confidence in such procedures could be provided through the modeling of theoretical atmospheres [55, 56]. Overall, ground-based measurements were difficult to execute and corrections for atmospheric contributions could overwhelm the measurement of interest, particularly as higher frequencies were examined. The emission from atmospheric water was easy to measure, as Smoot recalls in the "parking lot testing" of a radiometer at Berkeley: "*An invisible patch of water vapor drifted overhead; the scanner showed a rise in temperature. Good: this meant the*

instrument was working, because water vapor was a source of stray radiation" [21, p. 132].

The difficulty in obtaining quality measurements at high frequencies was directly associated with the presence of the water continuum, whose amplitude displays powerful frequency dependence [55, 56]. As a result, experiments were typically moved to locations where atmospheric water was minimized. Antarctica, with its relatively low atmospheric humidity, became a preferred monitoring location [55]. The same was true for mountain tops, places like Mauna Kea and Kitt Peak [55]. Many ground-based measurements were made from White Mountain in California, at an elevation of 3800 m [55]. But, there was one circumstance which should have given cosmologists cause for concern: measurements located near the oceans or a large body of water. These were amongst the simplest of all to perform. Weiss writes: "*Temperature, pressure, and constituent inhomogeneities occur and in fact are the largest source of random noise in ground-based experiments. However, they do not contribute systematic errors unless the particular observing site is anisotropic in a gross manner — because of a large lake or the ocean in the direction of the zenith scan, for example. The atmospheric and CBR contributions are separable in this case without further measurement or modeling*" [67, p. 500]. Surely, it might be of some importance that atmospheric contributions are always a significant problem which is only minimized when large bodies of condensed water are in the immediate scan direction.

The interesting interplay between atmospheric emissions and liquid surfaces is brought to light, but in a negative fashion, in the book by Mather [22]. In describing British work in the Canary Islands, Mather writes: "*Their job was unusually difficult because Atlantic weather creates patterns in the air that can produce signals similar to cosmic fluctuations. It took the English scientists years to eliminate this atmospheric noise...*" [22, p. 246–247]. As such, astronomers recognized that the Earth was able to alter their measurements in a substantial manner. Nonetheless, the possibility that condensed water itself was responsible for the microwave background continued to be overlooked.

1.4.2 U2 planes, rockets, and balloons

As previously outlined, the presence of water vapor in the lower atmosphere makes all measurements near the Wien maximum of the microwave background extremely difficult, if not impossible, from the ground. In order to gain more elevation, astrophysicists carried their instruments skywards using U2 airplanes, rockets, and balloons [21, 22]. All too often, these measurements reported elevated microwave background temperatures. The classic example is given by the Berkeley-Nagoya experiments, just before the launch of COBE [68]. Reflecting on these experiments, Mather writes: "*A greater shock to the COBE science team, especially to me since I was in charge of the FIRAS instrument, was an announcement made in early 1987 by a Japanese-American team headed by Paul Richards, my old mentor and friend at Berkeley, and Toshio Matsumoto of Nagoya University. The Berkeley-Nagoya group had launched from the Japanese island of Kyushu a small sounding rocket carrying a spectrometer some 200 miles high. During the few minutes it was able to generate data, the instrument measured the cosmic background radiation at six wavelengths between 0.1 millimeter and 1 millimeter. The results were quite disquieting, to say the least: that the spectrum of the cosmic microwave background showed an excess intensity as great as 10 percent at certain wavelengths, creating a noticeable bump in the blackbody curve. The cosmological community buzzed with alarm*" [22, p. 206]. The results of the Berkeley-Nagoya group were soon replaced by those from COBE. The origin of the strange "bump" on the blackbody curve was never identified. However, condensation of water directly into the Berkeley-Nagoya instrument was likely to have caused the interference. In contrast, the COBE satellite was able to operate in orbit, where any condensed water could be slowly degassed into the vacuum of space. COBE did not have to deal with the complications of direct water condensation and Mather could write in savoring the COBE findings: "*Rich and Ed recognized at once that the Berkeley-Nagoya results had been wrong*" [22, p. 216]. Nonetheless, the Berkeley-Nagoya experiments had provided a vital clue to the astrophysical community.

Water seemed to be constantly interferring with microwave experiments. At the very least, it greatly increased the complexity of studies performed near the Earth. For instance, prior to flying a balloon in Peru, Smoot reports: "*It is much more humid in the tropics, and as the plane descended from the cold upper air into Lima, the chilly equipment condensed the humidity into water. As a result, water collected into the small, sensitive wave guides that connect the differential microwave radiometer's horns to the receiver. We had to take the receiver apart and dry it... Our equipment had dried, so we reassembled it and tested it: it worked*" [21, p. 151].

Still, little attention has been shown in dissecting the underlying cause of these complications [6]. Drying scientific equipment was considered to be an adequate solution to address this issue. Alternatively, scientists simply tried to protect their antenna from condensation and added small monitoring devices to detect its presence. Woody makes this apparent, relative to his experiments with Mather: "*On the ground and during the ascent, the antenna is protected from atmospheric condensation by two removable windows at the top of the horn... At the same time, a small glass mirror allows us to check for atmospheric condensation in the antenna by taking photographs looking down the throat of the horn and cone*" [69, p. 16]. Indeed, monitoring condensation has become common place in detecting the microwave background using balloons. Here is a recent excerpt from the 2006 flight of the ARCADE 2 balloon: "*A video camera mounted*

on the spreader bar above the dewar allows direct imaging of the cold optics in flight. Two banks of light-emitting diodes provide the necessary illumination. The camera and lights can be commanded on and off, and we do not use data for science analysis from times when they are on" [70]. They continue: "*The potential problem with a cold open aperture is condensation from the atmosphere. Condensation on the optics will reflect microwave radiation adding to the radiometric temperature observed by the instrument in an unknown way. In the course of an ARCADE 2 observing flight, the aperture plate and external calibrator are maintained at cryogenic temperatures and exposed open to the sky for over four hours. Figure 12 shows time averaged video camera images of the dewar aperture taken two hours apart during the 2006 flight. No condensation is visible in the 3 GHz horn aperture despite the absence of any window between the horn and the atmosphere. It is seen that the efflux of cold boiloff helium gas from the dewar is sufficient to reduce condensation in the horn aperture to below visibly detectable levels*" [70].

The fact that condensation is not visible does not imply that it is not present. Microscopic films of condensation could very well appear in the horn, in a manner undetectable by the camera. In this regard, claims of strong galactic microwave bursts, reported by ARCADE 2 [70, 71] and brought to the attention of the public [72], must be viewed with caution. This is especially true, since it can be deduced from the previous discussion, that the camera was not functional during this short term burst. In any event, it is somewhat improbable that an object like the galaxy would produce bursts on such a short time scale. Condensation near the instrument is a much more likely scenario, given the experimental realities of the observations.

It remains puzzling that greater attention is not placed on understanding why water is a source of problems for microwave measurements. Singal et al. [70], for instance, believe that condensed water is a good reflector of microwave radiation. In contrast, our naval experiences, with signal transmission by submarines, document that water is an extremely powerful absorber of microwave radiation. Therefore, it must be a good emitter [8–12].

It is interesting to study how the Earth and water were treated as possible sources of error relative to the microwave background. As a direct precursor to the COBE FIRAS horn, it is most appropriate to examine the Woody-Mather instrument [69, 73]. Woody provides a detailed error analysis, associated with the Mather/Woody interferometer-based spectrometer [69]. This includes virtually every possible source of instrument error. Both Mather and Woody view earthshine as originating from a $\sim$300 K blackbody source. They appear to properly model molecular species in the atmosphere (H_2O, O_2, ozone, etc...), but present no discussion of the expected thermal emission profile of water in the condensed state on Earth. Woody [69, p. 99] and Mather [73, p. 121] do attempt to understand the response of their antenna to the Earth. Woody places an upper limit on earthshine [69, p. 104] by applying a power law continuum to model the problem. In this case, the Earth is modeled as if it could only produce 300 K photons. Such a treatment generates an error correction which grows with increasing frequency. Woody reaches the conclusion that, since the residuals on his fits for the microwave background are relatively small, even when earthshine is not considered, then its effect cannot be very significant [69, p. 105]. It could be argued that continental emission is being modeled. Yet, the function selected to represent earthly effects overtly dismisses that the planet itself could be producing the background. The oceans are never discussed.

Though Mather was aware that the water dimer exists in the atmosphere [73, p. 54], he did not extend this knowledge to the behavior of water in the condensed state. The potential importance of the hydrogen bond to the production of the microwave background was not considered [73]. At the same time, Mather realized that condensation of water into his antenna created problems. He wrote: "*The effect of air condensing into the antenna were seen...*" [73, p. 140]. He added: "*When the second window was opened, the valve which controls the gas flow should have been rotated so that all the gas was forced out through the cone and horn. When this situation was corrected, emissions from the horn were reduced as cold helium has cooled the surfaces on which the air had condensed, and the signal returned to its normal level*" [73, p. 140–141]. Mather does try to understand the effect of diffraction for this antenna [73, p. 112–121]. However, the treatment did not model any objects beyond the horn itself.

Relative to experiments with balloons, U2 airplanes, and rockets, the literature is replete with complications from water condensation. Despite this fact, water itself continues to be ignored as the underlying source of the microwave background. It is in this light that the COBE project was launched.

1.4.3 The central question

In studying the microwave background, several important conclusions have been reached as previously mentioned. First, the background is almost perfectly isotropic: it has essentially the same intensity, independent of observation angle [1]. Second, the background is not affected by seasonal variations on Earth [1]. Third, the signal is of thermal origin [8–17]. Finally, the background spectrum (see Figure 2) is clean: it is free from earthly interference. Over a frequency range spanning nearly 3 orders of magnitude ($\sim$1–660 GHz), the microwave background can be measured without any contaminating effect from the Earth. The blackbody spectrum is "perfect" [39]. But, as seen above, liquid water is a powerful absorber of microwave radiation. Thus, it remains a complete mystery as to why cosmology overlooked that the surface of the Earth could not produce any interference in these measurements. The only issue of concern for astrophysics is the atmosphere [55, 56] and its well-known absorption in the mi-

crowave and infrared bands. The contention of this work is that, if the Earth's oceans cannot interfere with these measurements, it is precisely because they are the primary source of the signal.

2 COBE FIRAS

For this analysis, the discussion will be limited primarily to the FIRAS instrument. Only a brief treatment of the DMR will follow in section 3. The DIRBE instrument, since it is unrelated to the microwave background, will not be addressed.

2.1 General concerns

Beginning in the late 1980's, it appeared that NASA would utilize COBE as a much needed triumph for space exploration [22, 24]. This was understandable, given the recent Challenger explosion [22, 24]. Visibility and a sense of urgency were cast upon the FIRAS team. COBE, now unable to use a shuttle flight, was faced with a significant redesign stage [22, 24]. Mather outlined the magnitude of the task at hand: "*Every pound was crucial as the engineers struggled to cut the spacecraft's weight from 10,594 pounds to at most 5,025 pounds and its launch diameter from 15 feet to 8 feet*" [22, p. 195]. This urgency to launch was certain to have affected prelaunch testing. Mather writes: "*Getting COBE into orbit was now Goddard's No. 1 priority and one of NASA's top priorities in the absence of shuttle flights. In early 1987 NASA administrator Jim Fletcher visited Goddard and looked over the COBE hardware, then issued a press release stating that COBE was the centerpiece of the agency's recovery*" [22, p. 194–195]. Many issues surfaced. These are important to consider and have been highlighted in detail [22, chap. 14].

After the launch, polite open dissent soon arose with a senior group member. The entire premise of the current paper can be summarized in the discussions which ensued: "*Dave Wilkinson, the FIRAS team sceptic, argued effectively at numerous meetings that he did not believe that Ned*" (Wright) "*and Al*" (Kogut) "*had proven that every systematic error in the data was negligible. Dave's worry was that emissions from the earth might be shinning over and around the spacecraft's protective shield*" [22, p. 234]. As will be seen below, Wilkinson never suspected that the Earth could be emitting as a $\sim$3 K source. Nonetheless, he realized that the FIRAS horn had not been adequately modeled or tested. Despite these challenges, the FIRAS team minimized Wilkinson's unease. Not a single study examines the interaction of the COBE shield with the FIRAS horn. The earthshine issue was never explored and Wilkinson's concerns remain unanswered by the FIRAS team to this day.

2.2 Preflight testing

A review of the COBE FIRAS prelaunch data reveals that the satellite was not adequately tested on the ground. These concerns were once brought to light by Professor Wilkinson, as mentioned above. He writes: "*Another concern was the magnitude of 300 K Earth emission that diffracted over, or leaked through, COBE's ground screen. This had not been measured in preflight tests, only estimated from crude (by today's standards) calculations*" [74]. Unfortunately, Professor Wilkinson does not give any detailed outline of the question and, while there are signs of problems with the FIRAS data, the astrophysical community itself has not published a thorough analysis on this subject.

Professor Wilkinson focused on the Earth as a $\sim$300 K blackbody source, even if the established behavior of the oceans in the microwave and far-infrared suggested that the oceans were not radiating in this manner [62]. Wilkinson never advanced that the Earth could be generating a signal with an apparent temperature of $\sim$3 K. This means that the diffraction problems could potentially be much more important than he ever suspected. Mather did outline Wilkinson's concerns in his book as mentioned above [22, p. 234], but did not elaborate further on these issues.

Beyond the question of diffraction, extensive testing of FIRAS, assembled in the flight dewar, did not occur. Mather stated that each individual component of FIRAS underwent rigorous evaluation [22, chap. 14], however testing was curtailed for the fully-assembled instrument. For instance, Hagopian described optical alignment and cryogenic performance studies for FIRAS in the test dewar [29]. These studies were performed at room and liquid nitrogen temperatures and did not achieve the cryogenic values, $\sim$1.4 K, associated with FIRAS [29]. Furthermore, Hagopian explained: "*Due to schedule constraints, an abbreviated version of the alignment and test plan developed for the FIRAS test unit was adopted*" [29]. Vibration testing was examined in order to simulate, as much as possible, the potential stresses experienced by FIRAS during launch and flight. The issue centered on optical alignments: "*The instrument high frequency response is however, mainly a function of the wire grid beam splitter and polarizer and the dihedrals of the MTM. The instrument is sensitive to misalignments of these components on the order of a few arc seconds*" [29]. In these studies, a blackbody source was used at liquid nitrogen temperatures to test FIRAS performance, but not with its real bolometers in place. Instead, Golay cell IR detectors were fed through light pipes mounted on the dewar output ports. It was noted that: "*Generally, the instrument behaved as expected with respect to performance degradation and alignment change... These results indicate that the instrument was successfully flight qualified and should survive cryogenic and launch induced perturbations*" [29]. These experiments did not involve FIRAS in its final configuration within the flight dewar and did not achieve operational temperatures.

A description of the preflight tests undergone by COBE was also presented by L. J. Milam [26], Mosier [27], and Co-

ladonato et al. [28]. These accounts demonstrate how little testing COBE actually underwent prior to launch. Concern rested on thermal performance and flight readiness. There obviously were some RF tests performed on the ground. In Mather [22, p. 216], it was reported that the calibration file for Xcal had been obtained on Earth. This was the file utilized to display the first spectrum of the microwave background with FIRAS [22, p. 216]. Nonetheless, no RF tests for sensitivity, side lobe performance, or diffraction were discussed for the FIRAS instrument. Given that Fixsen et al. [38] cite work by Mather, Toral, and Hemmati [25] for the isolated horn, as a basis for establishing side lobe performance, it is clear that these tests were never conducted for the fully-assembled instrument. Since such studies were difficult to perform in the contaminating microwave environments typically found on the ground, the FIRAS team simply chose to bypass this aspect of preflight RF testing.

As a result, the scientific community believes that COBE was held to the highest of scientific standards during ground testing when, in fact, a careful analysis suggests that some compromises occurred. However, given the scientific nature of the project, the absence of available preflight RF testing reports implies that little took place. Wilkinson's previously noted statement echoes this belief [74].

2.2.1 Bolometer performance

The FIRAS bolometers were well designed, as can be gathered from the words of Serlemitsos [31]: "*The FIRAS bolometers were optimized to operate in two frequency ranges. The slow bolometers cover the range from 1 to 20 Hz (with a geometric average of 4.5 Hz), and the fast ones cover the range from 20–100 Hz (average 45 Hz).*" Serlemitsos continues: "*The NEP's for the FIRAS bolometers are* $\sim 4.5\times10^{-15}$ *W/Hz*$^{1/2}$ *at 4.5 Hz for the slow bolometers and* $\sim 1.2\times10^{-14}$ *W/Hz*$^{1/2}$ *at 45 Hz for the fast ones*" [31], where NEP stands for "noise equivalent power". The FIRAS bolometers were made from a silicon wafer "*doped with antimony and compensated with boron*" [31]. Serlemitsos also outlined the key element of construction: "*IR absorption was accomplished by coating the back side of the substrate with metallic film...*" made "*of 20 Å of chromium, 5 Å of chromium-gold mixture, and 30–35 Å of gold*" [31]. Such vaporized metal deposits, or metal blacks, were well known to give good blackbody performance in the far IR [75,76]. Thus, if problems existed with FIRAS, it was unlikely that they could be easily attributed to bolometer performance.

2.2.2 Grid polarizer performance

The FIRAS team also fully characterized the wire grid polarizer [30]. While the grids did "*not meet the initial specification*" their spectral performance did "*satisfy the overall system requirements*" [30].

2.2.3 Emissivity of Xcal and Ical

The FIRAS team essentially makes the assumption that the two calibrators, Xcal and Ical, function as blackbodies over the entire frequency band. Xcal and Ical are represented schematically in Figure 3 [38, 42]. Both were manufactured from Eccosorb CR-110 (Emerson and Cuming Microwave Products, Canton, MA, 1980 [77]), a material that does not possess ideal attenuation characteristics. For instance, CR-110 provides an attenuation of only 6 dB per centimeter of material at 18 GHz [78]. In Hemati et al. [79], the thermal properties of Eccosorb CR-110 are examined in detail over the frequency range for FIRAS. The authors conduct transmission and reflection measurements. They demonstrate that Eccosorb CR-110 has a highly frequency dependent decrease in the transmission profile, which varies by orders of magnitude from $\sim$30–3,000 GHz [79]. Hemati et al. [79] also examine normal specular reflection, which demonstrate less variation with frequency. Therefore, when absorption coefficients are calculated using the transmission equation [79], they will have frequency dependence. Consequently, Hemati et al. [79] report that the absorption coefficients for Eccosorb CR-110 vary by more than one order of magnitude over the frequency range of FIRAS.

In addition, it is possible that even these computed absorption coefficients are too high. This is because Hemati et al. [79] do not consider diffuse reflection. They justify the lack of these measurements by stating that: "*For all samples the power response was highly specular; i.e., the reflected power was very sensitive with respect to sample orientation*" [79]. As a result, any absorption coefficient which is derived from the transmission equation [79], is prone to being overestimated. It is unlikely that Eccosorb CR-110 allows no diffuse reflection of incoming radiation. Thus, Eccosorb CR-110, at these thicknesses, does not possess the absorption characteristics of a blackbody. It is only through the construction of the "trumpet mute" shaped calibrator that blackbody behavior is thought to be achieved [38].

When speaking of the calibrators, Fixsen et al. [39] state: "*The other input port receives emission from an internal reference calibrator (emissivity* ≈ 0.98*)*" and "*During calibration, the sky aperture is completely filled by the external calibrator with an emissivity greater than 0.99997, calculated and measured*" [39]. Practical experience, in the construction of laboratory blackbodies, reveals that it is extremely difficult to obtain such emissivity values over a wide frequency range. Measured emissivity values should be presented in frequency dependent fashion, not as a single value for a broad frequency range [80]. In the infrared, comparable performance is not easily achievable, even with the best materials [15, 80]. The situation is even more difficult in the far infrared and microwave.

The emissivity of the calibrators was measured, at 34 and 94 GHz, using reflection methods as described in de-

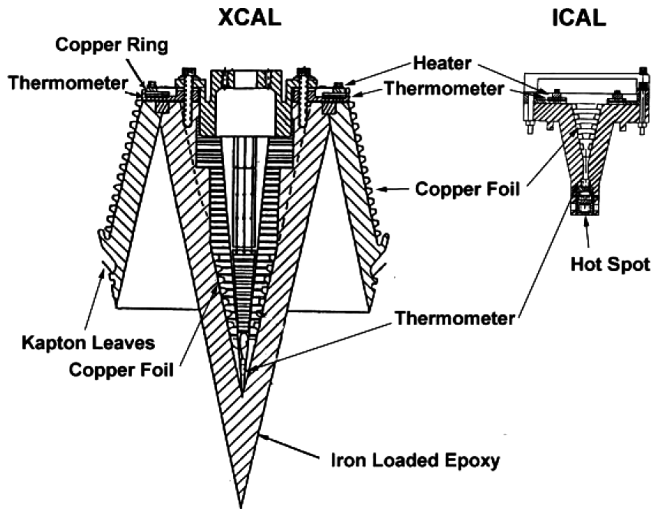

Fig. 3: Schematic representation of Xcal and Ical reproduced from [42]. Note that the calibrators are made from Eccosorb CR-110 which is backed with copper foil. Xcal, which contains three GRTs, is attached to the satellite with a movable arm allowing the calibrator to be inserted into, or removed from, the sky horn. The internal calibrator, Ical, is equipped with two GRTs and provides a signal for the reference horn. Reproduced by permission of the AAS.

tail [42]. However, these approaches are not appropriate for devices like the calibrators. In examining Figure 3, it is evident that Xcal is cast from layers of Eccosorb CR-110, backed with copper foil. For reflection methods to yield reliable results, they must address purely opaque surfaces. Eccosorb CR-110 is not opaque at these thicknesses [79] and displays significant transmission. The problem is worthy of further discussion.

In treating blackbody radiation, it is understood, from the principle of equivalence [8], that the emission of an object must be equal to its absorption at thermal and radiative equilibrium. Emission and absorption can be regarded as quantum mechanical processes. Therefore, it is most appropriate to state that, for a blackbody, or any body in radiative equilibrium, the probability of absorption, P_α, must be equal to the probability of emission, P_ε, $(P_\alpha = P_\varepsilon)$. But, given the combination of the transmittance for Eccosorb CR-110, the presence of a copper lining and the calibrator geometry, the FIRAS team has created a scenario wherein $P_\alpha \neq P_\varepsilon$. This is an interesting situation, which is permitted to exist because the copper backing on the calibrator provides a conductive path, enabling Xcal to remain at thermal equilibrium through non-radiative processes. Under these test conditions, Xcal is in thermal equilibrium, but not in radiative equilibrium. It receives incoming photons from the test signal, but can dissipate the heat, using conduction, through the copper backing. Xcal does not need to use emission to balance absorption.

If the FIRAS calibrators provide excellent reflection measurements [42], it is because of their "trumpet mute" shape and the presence of a copper back lining. Radiation incident to the device, during reflectance measurements, which is not initially absorbed, will continue to travel through the Eccosorb and strike the back of the casing. Here it will undergo normal specular reflection by the copper foil present at this location. The radiation can then re-enter the Eccosorb, where it has yet another chance of being absorbed. As a result, P_α can be effectively doubled as a consequence of this first reflection. Because of the shape of the calibrators, along with the presence of normal specular reflection on the copper, the radiation is essentially being pushed further into the calibrator where its chances of being absorbed are repeated. Consequently, P_α continues to increase with each reflection off the copper wall, or because photons are being geometrically forced to re-enter the adjacent Eccosorb wall. The situation moves in the opposite direction for P_ε and this probability therefore drops under test conditions.

Note that the copper foil has a low emissivity in this frequency range. Therefore, it is reasonable to assume that it cannot contribute much to the generation of photons. These must be generated within the Eccosorb CR-110 layers. Now, given the geometry of the "trumpet mute", there exists no means of increasing the probability of emission, P_ε. Indeed, some of the photons emitted will actually travel in the direction of the copper foil. This will lengthen their effective path out of the Eccosorb, since they exit and immediately re-enter, and increases the chance that they are absorbed before ever leaving the surface of the calibrator. Thus, P_ε experiences an effective decrease, because of the presence of the copper foil. The net result is that $P_\alpha \neq P_\varepsilon$ and the FIRAS team has not properly measured the emissivity of their calibrators using reflective methods [42]. In fact, direct measures of emissivity for these devices would demonstrate that they are not perfectly black across the frequencies of interest. Nonetheless, the devices do appear black in reflection measurements. But this is an illusion which does not imply that the calibrators are truly black when it comes to emission. Reflection measurements cannot establish the blackness of such a device relative to emission if the surface observed is not opaque. Geometry does matter in treating either emission or absorption under certain conditions. The problem is reminiscent of other logical errors relative to treating Kirchhoff's first proof for universality [16].

The FIRAS group asserts that they have verified the blackness of their calibrators with computational methods. Yet, these methods essentially "inject photons" into cavities, which otherwise might not be present [17]. Much like the improper use of detectors and reflection methods (on non-opaque surfaces), they can ensure that all cavities appear black [17]. The FIRAS calibrators are not perfectly black, but it is not clear what this implies relative to the measurements of the microwave background.

2.2.4 Leaks around Xcal

The acquisition of a blackbody spectrum from the sky is based on the performance of Xcal. For instance, Fixsen and Mather write: "*It is sometimes stated that this is the most perfect blackbody spectrum ever measured, but the measurement is actually the difference between the sky and the calibrator*" [43]. Mathematically, the process is as follows:

$$(\text{Sky} - \text{Ical}) - (\text{Xcal} - \text{Ical}) = (\text{Sky} - \text{Xcal}) .$$

Thus, Ical and all instrumental factors should ideally be negligible, contrary to what the FIRAS team experiences. Furthermore, if the calibration file with Xcal perfectly matches the sky, then a null result occurs. Since Xcal is thought to be a perfect blackbody, the derived sky spectrum is also ideal, as seen in Figure 2. It is extremely important that the calibration file, generated when Xcal is within the horn, does not contain any contamination from the sky. In the limit, should the sky dominate the calibration, a perfect blackbody shape will be recorded. This would occur because the sky is effectively compared against itself, ensuring a null.

The FIRAS team reminds us that: "*When the Xcal is in the sky horn it does not quite touch it. There is a 0.6 mm gap between the edge of the Xcal and the horn, so that the Xcal and the sky horn can be at different temperatures. Although the gap is near the flare of the horn and not in the direct line of sight of the detectors, it would result in undesirable leakage at long wavelengths because of diffraction. To ensure a good optical seal at all wavelengths, two ranks of aluminized Kapton leaves attached to the Xcal make a flexible contact with the horn*" [38] (see Figure 3). The claim that the Kapton leaves make a flexible contact with the horn, at operating temperatures, does not seem logical. The horn is operating at cryogenic temperatures ($\sim$2.7 K) and, thus, the Kapton leaves should not be considered flexible, but rather rigid, perhaps brittle. This might cause a poor contact with the horn during critical calibration events in space. The FIRAS team continues: "*An upper limit for leakage around the Xcal was determined in ground tests with a warm cryostat dome by comparing signals with the Xcal in and out of the horn. Leakage is less than 1.5×10^{-4} in the range $5 < \nu < 20$ cm^{-1} and 6.0×10^{-5} in the range $25 < \nu < 50$ cm^{-1}*" [38]. The issue of leakage around Xcal is critical to the proper functioning of FIRAS. Consequently, Mather et al. revisit the issue at length in 1999 (see section 3.5.1 in [42]). The seal does indeed appear to be good [42], but it is not certain that these particular ground tests are valid in space.

It is not clear if RF leak testing occurred while FIRAS was equipped with its specialized bolometers. As seen in section 2.2, in some preflight testing, Golay cell IR detectors had been fed through light pipes mounted on the dewar output ports. Such detectors would be unable to properly detect signals at the lowest frequencies. In fact, the FIRAS bolometers were made from metal blacks [31, 75, 76] in order to specifically provide sensitivity in the difficult low frequency range. As a result, any leak testing performed with the Golay cell IR detectors might be subject to error, since these may not have been sensitive to signal, in the region most subject to diffraction.

The FIRAS group also makes tests in flight and states: "*The Kapton levels sealing the gap between the sky horn and Xcal were tested by gradually withdrawing the Xcal from the horn. No effect could be seen in flight until it had moved 1.2 cm*" [38]. This issue is brought up, once again, by Mather et al.: "*A test was also done in flight by removing the calibrator 12 steps, or 17 mm, from the horn. Only a few interferograms were taken, but there was no sign of a change of signal level*" [42]. It is interesting that Fixsen et al. [38] claim that no effect could be seen until the horn had moved 1.2 cm. This implies that effects were seen at 1.2 cm. Conversely, Mather et al. assert that no effects were seen up to 17 mm [42]. In any case, identical results could have been obtained, even if the seal was inadequate. Perhaps this is why Fixsen et al. write: "*During calibration, the sky acts as a backdrop to the external calibrator, so residual transmission is still nearly 2.73 K radiation*" [39]. Clearly, if the seal was known to be good, there should not be any concern about "residual transmission" from the sky.

Fixsen et al. [39] rely on the sky backdrop providing a perfect blackbody spectrum behind Xcal. However, if the signal was originating from the Earth, the sky signal could be distorted as a function of frequency. This would bring error into the measurements, should the sky signal leak into the horn. From their comments, a tight seal by the Kapton leaves cannot be taken for granted. While in-flight tests, slowly removing Xcal, indicate that the spectrum changes as the calibrator was lifted out of the horn, they may not exclude that leakage exists when it is inside the horn.

It is also interesting that Mather describes significant problems with Xcal prior to launch, as follows: "*Now without gravity to help hold it in place, the calibrator popped out of the horn every time the test engineers inserted it by means of the same electronic commands they would use once COBE was in orbit. Nothing the engineers tried would keep it in place*" [22, p. 202]. In the end, the problem was caused by the flexible cable to the Xcal [22]. The cable was replaced with three thin ribbons of Kapton [22, p. 202–204]. COBE underwent one more cryogenic test, with the liquid helium dewar at 2.8 K, lasting a total of 24 days ending in June 1989 [26]. Milan's report does not provide the results of any RF testing [26], but everything must have worked. The satellite was prepared for shipment to the launch site [22, p. 202–204].

In 2002, Mather reminds us of the vibration problems with COBE: "*There were annoying vibrations at 57 and ~ 8 Hz*" [43]. On the ground, the Xcal could "pop out" of the horn if the satellite was turned on its side [22, p. 202]. Only gravity was holding Xcal in place. Still, in orbit, COBE experiences very little gravity. As such, the effects of the vi-

brations in knocking Xcal out of the horn, or in breaking the contact between the Kapton leaves and the horn, are not the same in space. A small vibration, in space, could produce a significant force against Xcal, pushing it out of the horn. Thus, all leak testing on the ground has little relevance to the situation in orbit, since both gravity and vibrations affect the Xcal position in a manner which cannot be simulated in the laboratory. The FIRAS team simply cannot be assured that Xcal did not allow leakage from the sky into the horn during calibration.

2.2.4.1 Conclusive proof for Xcal performance

When FIRAS first begins to transfer data to the Earth, a calibration file using Xcal had not been collected in space [22, p. 216]. Nonetheless, a calibration file existed which had been measured on the ground. Mather provides a wonderful account of recording the first blackbody spectrum from the microwave background [22, p. 216]. The text is so powerfully convincing that it would be easy to dismiss the search for any problems with FIRAS. Using the ground-based calibration file, the FIRAS team generates an "*absolutely perfect blackbody curve*" [22, p. 216]. However, considering all of the errors present in orbit, it is not clear how the calibration file gathered on Earth differed, if at all, from the one obtained in space. If the FIRAS team had wanted to bring forth the most concrete evidence that the situation in space, relative to Xcal, was identical to that acquired on the ground, then they could have easily displayed the difference spectrum between these two files. Ideally, no differences should be seen. But, if differences were observed, then either temperature variations, or leakage, must be assumed. In fact, the difference between the two files could have provided a clue as to the nature of the leakage into the FIRAS horn. Mather et al. feel compelled to verify the performance of Xcal on the ground 10 years after launch [42]. This suggests that the calibration files taken prior to launch did not agree with those acquired in flight.

2.2.5 Design of the FIRAS horn

In examining the FIRAS horn (see Figure 1), it is apparent that this component does not conform to accepted practices in the field of antenna design [81–83]. This device is unique, meant to operate over a phenomenal range from ∼30 to 3,000 GHz [32–45]. Since broadband horns generally span no more than 1 or 2 decades in frequency [84, 85], it is doubtful that a comparable antenna can be found in the electromagnetics literature. Even the most modern broadband horns tend to cover very limited frequency ranges and, typically, at the expense of variable gains across the band [84, 85]. Unfortunately, insufficient ground tests were conducted, to demonstrate the expected performance from 30–3,000 GHz. It is highly unlikely that FIRAS was ever able to perform as intended. The FIRAS team provides no test measurements to the contrary. These would have included gain and side lobe performances spanning the frequency spectrum. Moreover, as will be seen below (see section 2.4.3.1), FIRAS is operating less than optimally over all wavelengths. The idea of using an interferometer for these studies was elegant [32–45]. But, broadband horns with demonstrated performances, over such a range of frequencies, simply do not exist [81–85]. It is interesting in this light, that the WMAP [19] and PLANCK [86] missions have both reverted to the use of narrow band devices to sample the microwave background. As for FIRAS, it functions primarily from ∼30–600 GHz. However, even in this region, the instrument must deal with horn/shield interactions and the effects of diffraction. These effects were never appropriately considered by the FIRAS team.

The testing of the COBE FIRAS antenna pattern was inadequate. Proper tests were never performed to document the interaction of the FIRAS horn with the Sun/Earth/RFI shield. Furthermore, the team conducted no computational modeling of the horn-shield interaction as a function of frequency. This type of documentation would have been central in establishing the reliability of the FIRAS findings. Without it, the FIRAS team did not eliminate the possibility that the Earth itself is producing the microwave background. The RF shield on COBE could accomplish little more than prevent terrestrial/solar photons, in the visible or near-infrared range, from directly illuminating the dewar which contains FIRAS. The central issue for the Sun/Earth shield appears to be the conservation of helium in the dewar, not the elimination of RF interference [87]. The shield is not corrugated [81, p. 657–659] and has no special edges to prevent diffraction in the far infrared. Given that the FIRAS horn is broadband, it is extremely difficult, if not impossible, to build a good RF shield for such a device. The FIRAS team has not established that an adequate shield was constructed to prevent RF interference from the Earth. The Sun/Earth shield simply prevents direct heating of the dewar, by visible or near infrared light [87]. They comment: "*a large external conical shield protects the cryostat and instruments from direct radiation from the Sun and the Earth. The Sun never illuminates the instruments or cryostat, but the COBE orbit inclination combined with the inclination of the Earth's equator to the ecliptic do allow the Earth limb to rise a few degrees above the plane of the instrument and sunshade apertures during about one-sixth of the orbit for one-fourth of the year. During this period, the sky horn could not be cooled to 2.7 K because of the Earth limb heating*" [42]. Nowhere, in the COBE literature, is the RF performance of the "sunshade" analyzed.

2.3 FIRAS in flight

2.3.1 Side lobe performance

Fixsen et al. [38] argue that the FIRAS horn "*provides a 7° field of view with low side lobes*". They base this statement on work by Mather, Toral, and Hemmati [25]. In this paper, Mather et al. present measured and theoretical evaluations of

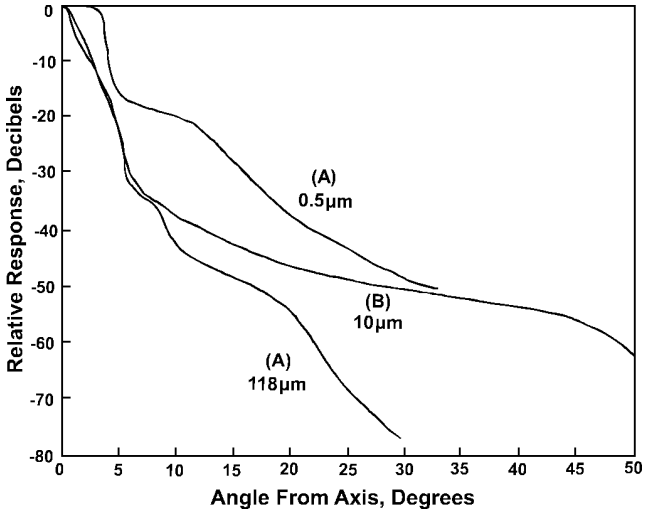

Fig. 4: Plot of the side lobe response for the FIRAS horn, without the presence of the COBE ground shield as reproduced from [25]. The sky lobe response, in preflight testing, was evaluated at three wavelengths, namely 118, 10, and 0.5 μm. Note that only the first measurement at 118 μm ($\sim$2,540 GHz) is within the frequency range of the instrument (30–3000 GHz). The latter two occur in the optical band. The side lobe performance is best at the longer wavelength, in opposition to the expected theoretical result. The FIRAS team also measures the FIRAS horn at 31.4 and 90 GHZ [25], with excellent performance (data is not reproduced herein). However, once again, these results were obtained without the interfering effects of the ground shield. Reproduced with permission of the Optical Society of America from: Mather J.C., Toral M., Hemmati H. Heat trap with flare as multimode antenna. *Appl. Optics*, 1986, v. 25(16), 2826–2830 [25].

side lobe data at 31.4 and 90 GHz [25]. As expected, the side lobes are lower at the higher frequency. The measurements conform to expected performance, at least at these frequencies. But, these tests were conducted without the RF shield and consequently have limited relevance to the actual situation in flight.

A careful examination of Figure 4 [25] is troubling. In this figure, Mather et al. [25] characterize the antenna pattern of the isolated FIRAS horn, without the COBE RF shield, at infrared and optical wavelengths (118, 10, and 0.5 μm). It is not evident why the authors present this data, as only the first wavelength, 118 μm ($\sim$2,540 GHz), is within the usable bandwidth of the instrument. Nonetheless, in Figure 4, the antenna has the strongest side lobes at the highest frequencies. For instance, at a wavelength of 0.5 μm, the antenna shows a relative response that is decreased by only 20 dB at 10° [25], as shown in Figure 4. At 118 μm, the antenna response is decreased by nearly 50 db. The authors are demonstrating that the FIRAS horn has better side lobe behavior at longer wavelengths rather than at short wavelengths. This is opposed to the expected performance. Mathematical modeling may well be impossible at these elevated frequencies. Once again, the shield was never considered.

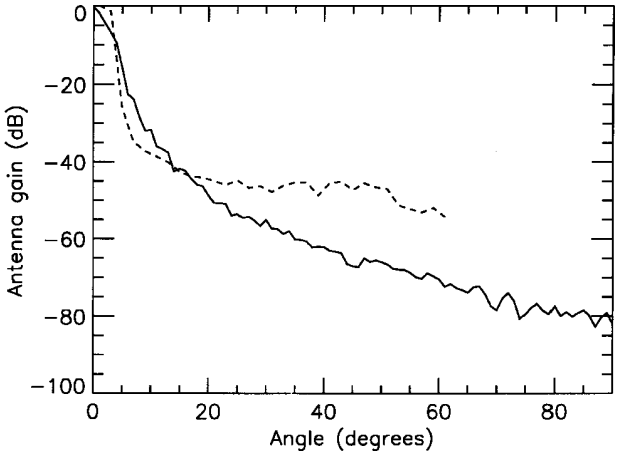

Fig. 5: Plot of the side lobe response obtained for the FIRAS shield on the ground, at 3 cm^{-1} (solid line), and in orbit, using the Moon as a source of signal, at 50 cm^{-1} (dashed line). This figure is reproduced from [38]. A detailed discussion is provided in section 2.3.1. Reproduced by permission of the AAS.

Neglecting to characterize the horn-shield interaction on the ground, the FIRAS team attempts to do so in flight. In Fixsen et al. [38], they publish Figure 5. They attempt to determine the antenna pattern in space by monitoring the Moon as a function of angle. Using this approach at 50 cm^{-1}, they conclude that the satellite provides a maximum side lobe response of "*less −38 dB beyond 15° from the center of the beam*" [38]. Such a performance is reasonable, at least at this frequency. However, the FIRAS team then compares side lobe performance at 50 cm^{-1} ($\sim$1,500 GHz) with data obtained on the ground at 3 cm^{-1} ($\sim$90 GHz). In referring to this figure in their paper, the FIRAS team writes: "*Preliminary results are shown in Figure 4, along with preflight measurements at 1 and 1.77 cm^{-1}*" [38]. Yet the figure legend itself states the following: "*Antenna pattern for the FIRAS horn as measured on the ground before launch at 3 cm^{-1} (solid line) and as measured from in flight Moon data at $\sim$50 cm^{-1} (dashed line)*" [38]. Beyond the inconsistency between the text and the figure legend, there are at least five concerns relative to this figure.

First, the data on the ground appears to have measured the FIRAS horn exclusively, not the horn with the RF shield. Second, they are comparing data at frequencies which differ by more than one order of magnitude. Third, they display none of the critical in-flight data for the lowest frequencies, namely those frequencies where one would expect the strongest effects from diffraction. Fourth, they fail to present ground data at 50 cm^{-1}. Finally, the data from Fixsen et al. [38] is also puzzling. It reveals much stronger side lobes at 50 cm^{-1} than one would have predicted at this frequency ($\sim$1,500 GHz). Note, in Figure 5, that the Moon data displays a plateau at approximately -45 dB in the range from 20–50°. This is higher than would be expected, based on the excellent side lobe response, even at a much lower 90 GHz, reported for the free

horn on the ground [25]. This plateau may simply be caused by a lack of sensitivity for the Moon at these angles. It is impossible to determine whether the plateau achieved in detection is a result of this effect. The FIRAS Explanatory Supplement suggests that the Moon can contaminate the microwave background at all frequencies [40, p. 61]. The FIRAS team does not adequately confront the issue and does not publish a work focused on side lobe behavior. Comparing ground data at ∼30 GHz, or even ∼90 GHz, with in-flight data at 1,500 GHz, has no value relative to addressing the side lobe issue.

It is also true that a loss of "Moon signal", as a function of angle, could account for the appearance of good side lobe performance. The possibility that the Moon could be reflecting terrestrial, or even solar, signals back into the FIRAS horn, through normal specular reflection, is not discussed. This process would be angle dependent and might create the illusion of reasonable side lobe behavior. The FIRAS team provides no supportive evidence from the literature that the Moon behaves as a lambertian emitter at 50 cm^{-1}. The Moon does have phases, which result in differential heating across its surface. Should the Moon not act as a lambertian emitter, the side lobe performance was not properly evaluated. This would be true, unless the satellite was rapidly turned away from the Moon while maintaining a single orbital position. But, this is unlikely to have been the case, since COBE did not have a propulsion system [22, p. 195]. Thus, the satellite was simply permitted to continue in its orbit, and the angle to the Moon thereby increased. Such a protocol might not accurately assay side lobe behavior. This is because it would depend on the absence of specular reflection from the Earth and the Sun, while requiring that the Moon is lambertian. In the end, experiments in space cannot replace systematic testing on the ground in establishing side lobe behavior.

Perhaps more troubling is that the frequencies of interest, relative to the microwave background, extend from less than 1 cm^{-1} to ∼22 cm^{-1} (<30 to ∼660 GHz). For example, the initial Penzias and Wilson measurements were made near 4 GHz [1]. Consequently, the FIRAS team is showing side lobe performance for a region outside the frequencies of interest. In fact, 1,500 GHz is the region wherein galactic dust would be sampled, not the microwave background [23]. The side lobe performance at this frequency is not relevant to the problem at hand. Furthermore, if there are problems with diffraction, they are being manifested by a distortion of signal, primarily in the lower frequency ranges. Hence, it would be critical for the FIRAS team to display in-flight data, or ground data including the shield, in order to fully document side lobe performance in this region. The data, unfortunately, is not provided.

Should access be available to the exact dimensions of the FIRAS horn and the COBE shield, it would, in principle, be possible for an independent group to verify the performance of the satellite relative to this instrument. It is true that the problem of modeling the FIRAS horn/shield interaction is extremely complex, even at 30 GHz. Nonetheless, given current computational methods, using the Geometric Theory of Diffraction, it is difficult to reconcile that the true directional sensitivity of the FIRAS horn was not modeled at any frequency. These studies would depend on obtaining the exact configuration, for the FIRAS horn/shield, and then treating the problem using computational methods. The issue cannot be treated analytically. Furthermore, this is a difficult task. It is achievable perhaps, only at the lowest frequencies of operation.

In 2002, Fixsen and Mather give a summary of the FIRAS results [43], wherein they also describe how a new instrument might be constructed. In order to address the lack of side lobe characterization, they advance that: "*we would surround the entire optical system with segmented blackbody radiators to measure the side lobe responses and ensure that the source of every photon is understood*" [43]. With COBE, the source of every photon was not understood. The side lobes were never measured in the presence of the shield. The idea of surrounding the optical system with blackbody calibrators is less than optimal. It would be best to simply analyze the horn/shield performance with preflight testing.

2.3.2 Establishing temperatures

The FIRAS team presents a dozen values for the microwave background temperature, using varying methods, as shown in Table 1. This occurs over a span of 13 years. Each time, there is a striking recalculation of error bars. In the end, the final error on the microwave background temperature drops by nearly two orders of magnitude from 60 mK to 0.65 mK. Yet, as will be seen below, in sections 2.3.3 and 2.3.4, FIRAS was unable to yield proper nulls, either with the sky and Ical, or with Xcal and Ical. Despite the subsequent existence of systematic errors, the FIRAS team minimizes error bars.

The problems with correctly establishing temperatures for Xcal and Ical were central to the mission, as these investigators recognized: "*There were two important problems. One was that the thermometers on both the Ical and Xcal did not at all agree. In fact, the disagreement among different Xcal thermometers was 3 mK at 2.7 K*" [38]. They continue: "*The disagreement between the Ical thermometers was 18 mK at 2.7 K. The heat sinking of the Ical thermometer leads was inadequate, and some of the applied heat flowed through part of the Ical*" [38].

They try to overcome the reality that the temperature monitors on the external calibrator report a systematic error. The temperature errors on Xcal are fitted with an "*arbitrary offset in the Xcal thermometer and the result was* -7.4 ± 0.2 *mK for this offset*" [38]. The FIRAS team realizes that this was "*considerably larger than the ∼1 mK expected from the preflight calibration of the thermometers*" [38]. They attribute the problem either to having improperly calibrated the thermometers before flight, or due to an unknown systematic

Reference	Temperature	Error (mK)*	Frequency (cm^{-1})
Mather et al., *ApJ*, 1990, v. 354, L37–40 [32]	2.735§	±60	1–20#
Mather et al., *ApJ*, 1994, v. 420, 439–444 [35]	2.726§	±10	2–20#
Fixsen et al., *ApJ*, 1996, v. 473, 576–587 [39]	2.730§	±1	2–21†
Fixsen et al., *ApJ*, 1996, v. 473, 576–587 [39]	2.7255¶	±0.09	2–21†
Fixsen et al., *ApJ*, 1996, v. 473, 576–587 [39]	2.717¥	±7	2–21†
Fixsen et al., *ApJ*, 1996, v. 473, 576–587 [39]	2.728**	±4	2–21†
Mather et al., *ApJ*, 1999, v. 512, 511–520 [42]	2.725§	±5	2–20‡
Mather et al., *ApJ*, 1999, v. 512, 511–520 [42]	2.7255¶	±0.085	2–21†
Mather et al., *ApJ*, 1999, v. 512, 511–520 [42]	2.722¥	±12	2–20‡
Mather et al., *ApJ*, 1999, v. 512, 511–520 [42]	2.725**	±2	2–20‡
Fixsen & Mather, *ApJ*, 2002, v. 581, 817–822 [43]	2.725	±0.65	2–20‡
Fixsen & Mather, *ApJ*, 2002, v. 581, 817–822 [43]	2.725	±1	2–20‡

* 95% confidence intervals.
§ Measurement using FIRAS microwave background lineshape. Calibration sensitive to the thermometers of the external calibrator, Xcal.
¶ Measurement using FIRAS microwave background frequency. Calibration relies on CO and C+ lines at 7.69, 11.53, 15.38, and 16.42 cm^{-1} [39].
¥ Measurement using a fit of the dipole spectrum to the 1st derivative of a Planckian function describing the microwave background with T_{cmbr} set to 2.728 K.
** Composite value obtained from analysis of three previous entries.
# Frequency range used is formally stated.
† Frequency range used is not formally stated but appears to be 2–21 cm^{-1}.
‡ Frequency range used is not formally stated but appears to be 2–20 cm^{-1}.

Table 1: Summary of microwave background temperatures obtained by the COBE FIRAS instrument.

error. They therefore assign a -4 mK offset to Xcal and raise to 5 mK its 1σ error. Though this might seem negligible, the FIRAS team is sufficiently concerned about Xcal that they attempt to recalibrate it on the ground, using a duplicate experiment, nearly ten years after launch [42]. For the present discussion, an error of at least 5 mK can be attributed to Xcal.

The FIRAS Explanatory Supplement outlines an enhanced picture relative to Ical performance [40, p. 42]. An optical temperature drift is modeled as follows:

$$T' = T + A \exp\left(t/\tau_{\mathrm{Ical}}\right) + T_{\mathrm{offset}}$$

where T' is the "raw" Ical temperature, $A = 4.26$ mK, $T_{\mathrm{offset}} = -3.054$ mK, and $\tau_{\mathrm{Ical}} = 104.3$ days [40, p. 42]. Given that FIRAS was operational for ∼259 days [40, p. 28], the drift model accounts for a 48 mK error in Ical by the time the instrument is decommissioned. Yet, in 1999, Mather et al. [42] offer a different view [40, p. 42]. While treating Ical, they write: "*An additional drift of ∼3 mK was noted in the early part of the mission*" [42]. Thus, it is likely that the equation in the supplement is simply missing a negative sign in the exponent. As a result, the ∼3 mK drift, discussed by Mather et al., can be attributed to Ical [42] along with errors of 18 mK for temperature differences between thermometers. In addition, as demonstrated in Figure 6, the emissivity modeled for Ical can exceed the theoretical upper limit of 1 over much of the FIRAS frequency range. This illustrates that the calibration model adopted by the FIRAS team contains significant shortcomings.

2.3.3 Achieving a sky null

As represented in Figure 1, FIRAS functions as a differential spectrometer, wherein the sky or the external reference, Xcal, are being constantly compared to an internal reference blackbody, Ical. When the system is functioning properly and all temperatures are equal, then a perfect null should be measured in the interferogram. This should take place whether 1) the sky is being compared to Ical set at the temperature of the sky, or 2) the external reference calibrator, Xcal, is being compared to Ical set at the same temperature.

Once COBE finally reaches orbit, the first finding is that FIRAS is unable to achieve a null when the internal reference Ical is set to the sky temperature. This is demonstrated in Figure 7 [32]. Years later, the FIRAS team discuss the situation: "*If both the sky and the Ical were blackbodies, and the interferometer were perfectly symmetrical, one could in principle null the signal from the former simply by adjusting the temperature of the latter. The temperature of the CMBR could then be read from the reference body thermometers. Unfortunately, neither of those conditions prevails*" [38]. The FIRAS team continues: "*Our Ical and instrument asymmetry com-*

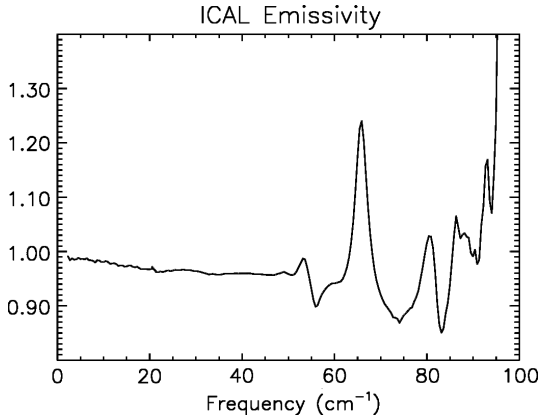

Fig. 6: Calculated emissivity for Ical as a result of calibration reproduced from the FIRAS Explanatory Supplement [40]. Note that emissivity exceeds 1, the theoretical maximum, at many frequencies. Reprinted with permission of John Mather.

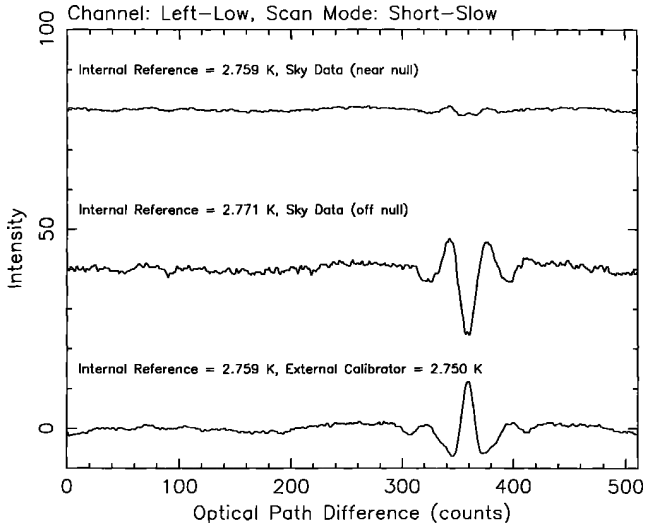

Fig. 7: Interferograms obtained in flight with the FIRAS instrument, as reproduced from [32]. The upper trace demonstrates the null condition between the sky (final reported temperature = 2.725±0.001 K [43]) and Ical set at 2.759 K. This trace is not plotted with the same vertical scaling factor as the one displayed in the central portion of the figure. Such a plot creates the illusion that a better result was achieved than actually obtained. The middle trace displays the interferogram recorded when Ical was set at 2.771 K. This indicates the magnitude of signal "off the null". The bottom interferogram was measured when comparing the two calibrators set at nearly the same temperature (Xcal = 2.759; Ical = 2.750). A null should have been obtained under these conditions, but did not occur. Once again, the vertical scale does not correspond to that used for the central trace. A correction of a factor of 3–5 should be applied to place the upper and lower interferograms on scale with the central one. This was not mentioned in the original text [32], but points to deviations from the theoretically expected results. Reproduced by permission of the AAS.

bine to produce a net reflectance of ∼4%, and Galactic emission from gas and dust contributes to the observed signal. To measure these effects, we must calibrate the instrument" [38]. Note that since the sky temperature would end up being assigned as 2.725±0.001 K [43], the upper trace in Figure 7 indicates that the null point appears with Ical at nearly 34 mK above the sky temperature (2.759–2.725 K = 34 mK). Consequently, COBE is faced with a 34 mK systematic error based on this fact. It is not clear how much of this error can be attributed to Galactic emissions. These should be primarily sensed at frequencies beyond 20 cm^{-1} [23], the cutoff of the low frequency channel [38]. As such, it is doubtful that galactic contributions can fully account for the lack of a proper null in these channels. By the end of the mission, Ical is spending most of its time near the null, at ∼2.758 K and toggling to a temperature 12 mK higher, ∼2.770 K [40, p. 28]. The FIRAS team writes: "*In addition, the temperature of Ical was toggled between a "sky null" setting to a setting 12 mK hotter, every 3–4 days, to allow instrumental gain errors to be distinguished*" [40, p. 19]. The latter is 45 mK above the temperature reported for the microwave background.

Unable to attain the expected null, the FIRAS team begins to target instrumental problems and calibration [38]. They do not envision that a null could not be achieved, because the sky was not acting as anticipated. Consider, for instance, that the Earth is producing the microwave background and that its diffracted signal is coming over the shield of the satellite. In this case, one can assume that the Earth was producing a signal with a nearly perfect Planckian [10] shape. But, at lower frequencies, the microwave background will experience more diffraction at the shield. Hence, FIRAS will be most sensitive to low frequency signals. As frequencies are increased, progressively less diffraction will occur at the shield and the FIRAS horn will become more forward directional. In so doing, it will be less sensitive to signals arising from beneath the shield. Thus, FIRAS may not sense a true Planckian curve, but a distorted spectrum displaying too much signal at the lower frequencies, and not enough signal at the higher frequencies. There may be less than the expected signal instensity along with constructive/destructive interference effects. The situation is illustrated schematically in an exaggerated fashion in Figure 8. This scenario would make it impossible to reach a null. The issue is not simply a question of temperature, but of lineshape. If two signals, arising from the sky and Ical, do not have the same lineshape, they can never be nulled. A proper null is never displayed. The underlying cause cannot be ascertained, given the nature of preflight testing, instrumental drift, and incoming signal.

In re-examining Figure 7 [32], note that the trace determining the null point is not a good null. The top trace in this figure is not plotted on the same scale as the bottom two traces, as can be deduced by examining the noise power. It needs to be multiplied by a factor of 3–5 to match the noise seen in the central trace. This gives the illusion that a better null is achieved than is actually obtained in practice. The second trace has much more noise. In fact, an analysis of noise

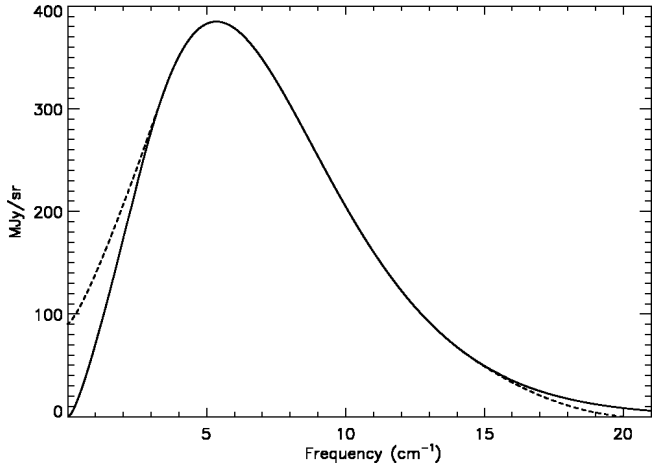

Fig. 8: Schematic representation of an ideal blackbody at 2.725 K (solid line). The dashed line is an exaggerated representation of the distortions that might occur if an earthly signal was diffracting over the FIRAS ground shield. Since diffraction might be expected to have the greatest effects at the lowest frequencies, the points in this region would be elevated. Conversely, as frequencies are increased, less diffraction should occur off the ground shield. The FIRAS horn should become more forward directional at elevated frequencies. As a result, a decreased signal might be sensed in this region. It is difficult to deduce the exact appearance of the effects from diffraction. For instance, there could actually be signs of constructive and destructive interference on the acquired spectrum. The nature of the spectrum acquired by FIRAS would also depend on the extent that the sky signal was diffracting into the FIRAS horn during calibration with Xcal, due to leakage. In the limit of severe leakage, FIRAS would report a perfect blackbody spectrum from the sky, even with diffraction occurring at the ground shield. Further details are provided in the text.

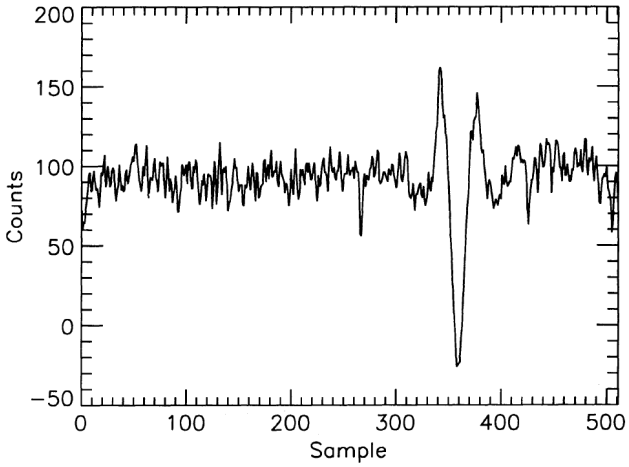

Fig. 9: FIRAS interferogram acquired between the sky and Ical, as reproduced from [38]. The signal is being generated just slightly "off the null". Apparently, the point at 355 can be perfectly nulled [38], but it is doubtful that such a result can be obtained while maintaining the null condition over all other points. The FIRAS team does not present a perfect null. A spectrum acquired "just off the null" yields little scientific information. Reproduced by permission of the AAS.

power from these traces establishes that the FIRAS team is not maintaining a constant vertical amplification. This should not have escaped the eye of the reviewers. Correct scaling factors should have been provided in the figure legend.

In any case, the null is not clean. The FIRAS team, for instance, shows a second interferogram in Fixsen et al. [38], reproduced herein as Figure 9. In the figure legend, they state that the peak at 355 can be nulled within detector noise levels. However, they fail to demonstrate the corresponding interferogram. It is certain that the point at 355 can be nulled. But, it is essential that all the points in the spectrum are simultaneously nulled. The FIRAS team has never been able to present such an interferogram. Moreover, if a proper null exists, they should not display data "just off the null". These interferograms are not useful as measures of instrument performance. The issue is not simply one of temperature match. For, if two blackbodies are brought to the same temperature, then ideally, the null must be perfect. Lineshape differences, generated by diffraction on the shield, could account for the discrepancies noted.

Unable to reach a perfect null with the sky and dismissing lineshape effects, the FIRAS team is left to implicate instrument design [38]. This is because they believe that a perfectly Planckian background must be found in the sky in front of FIRAS. The idea that an ideal blackbody spectrum, produced by the Earth, could have been distorted by diffraction over the shield, is not entertained. As a result, they cite that the Ical provides a 4% reflectance, to partially account for the lack of a proper null [38].

2.3.4 Achieving a null when $T_{\mathrm{Ical}} = T_{\mathrm{Xcal}}$

In analyzing the bottom trace in Figure 7, it is evident that a null cannot be achieved, when Xcal is set at nearly the same temperature as Ical (Xcal = 2.750 K, Ical = 2.759 K). Unfortunately, the FIRAS team does not publish a sufficient number of interferograms to enable the complete dissection of this question. On the surface, failure to locate a null, when $T_{\mathrm{Ical}} = T_{\mathrm{Xcal}}$, would support the idea that the problem was instrumental. After all, a second failure to establish a solid null is being reported. The FIRAS team might have been able to supply proof of this contention, using a combination of interferograms with Xcal and Ical at differing temperatures. As it is, no proof exists that Ical was the sole problem with FIRAS. Again, failure to attain a null, when $T_{\mathrm{Ical}} = T_{\mathrm{Xcal}}$, could also be supported by technical issues with leakage around Xcal.

It is vital to understand the exact temperatures for Xcal and Ical, when a null spectrum is achieved by the two calibrators. However, such data is not presented by the FIRAS team. Furthermore, it is not certain that they were ever able to obtain a null. In order to properly address this issue, the critical data is found in the null spectrum between Xcal and Ical on the ground. It is not known if the null imbalance was documented for FIRAS using preflight tests. The data have

not been published, but are critical to understanding the inability to reach a null between the sky and Ical, as discussed in section 2.3.3. Without it, the FIRAS team cannot defend the hypothesis that galactic contributions, for instance, were responsible for this shortcoming. It is obvious that the galaxy may not be invoked for the lack of a null between the two reference blackbodies. Therefore, for a proper evaluation of these questions, ground data, obtained between Xcal and Ical, should be provided.

2.4 Data processing

Initially, the FIRAS team publishes a spectrum from 1–21 cm^{-1} [32]. That spectrum was said to deviate from the intensity of a blackbody by less than 1%. Then, in 1994, Mather et al. [35] advance a new set of data, wherein the intensity deviates from a blackbody by less than 0.03%. The error bar in setting the absolute temperature, using Xcal, drops precipitously from 60 mK to 10 mK (see Table 1). Fixsen et al. [39], in 1996, then report that the "*rms deviations are less than 50 parts per million of the peak of the cosmic microwave background radiation*". In 1999, Mather et al. apparently again increase the rms deviation and assert that the deviation of the CMB from the theoretical blackbody is less than 0.01% [42]. Finally, in 2002, Fixsen and Mather [43] advance that "*the measured deviation from this spectrum are 50 parts per million (PPM, rms) of the peak brightness of the CMBR spectrum, within the uncertainty of the measurement*". Using technology established in the 1970's, the FIRAS team reported a spectral precision well beyond that commonly achievable today in the best radiometry laboratories of the world.

Figure 2 [39] is famous for the observation that the uncertainties are a small fraction of the line thickness. This figure is unusually drawn, as the frequency axis is offset. This makes it less apparent that data is not being shown below 2 cm^{-1}. The final result was obtained with the calibration procedures outlined by Fixsen et al. [38]. In the end, the FIRAS team transfers the error from the spectrum of interest into the calibration file, as will be discussed in detail below. Using this approach, it would be possible, in principle, to attain no deviations whatsoever from the perfect theoretical blackbody. Given enough degrees of freedom and computing power, errors begin to lose physical meaning. The calibration file became a repository for everything that did not work with FIRAS. The only problem was that it was now impossible to dissect what the FIRAS microwave background spectrum really looked like. Along these lines, the most serious concern was the omission of data, as discussed in section 2.4.3.

2.4.1 FIRAS calibration

In order to provide data for in-flight calibration, the FIRAS team controls the temperature of four key sources of emission, 1) the internal calibrator, 2) the external calibrator, 3) the sky horn, and 4) the reference horn. The emissivity of each of these devices could be modified on demand in the temperature range from 2–25 K [38]. Other parts of the instrument are approximated as Planckian functions [10], presumably because they are isothermal [38]. Cheng describes the calibration process: "*Calibration is accomplished by removing all known instrument effects from the raw spectra. This requires a model of the instrument, with all known imperfections, and sufficient calibration data to establish the model parameters. The measured instrument state for the sky data can then be used to predict the instrument characteristics based on the model which is then used to calibrate the sky data... The emissivity of various internal components in the instrument are determined by varying their temperatures while observing a constant input signal (e.g. from the external calibrator). These components include the sky horn, reference horn, internal reference load, dihedral mirrors, collimator, and the detector itself. The temperature of the first three components can be varied by command so that determining their emissivity is straightforward. The emissivity of the other components are determined by temperature variations during several cryostat temperature transients which occurred early on in the mission*" [34].

A critical aspect of the calibration procedure is that the external calibrator, Xcal, is treated as providing a perfect blackbody signal to the rest of the instrument. This approximation may not be justified, given the discussion in section 2.2.3. There are also complications, if the seal between the horn and the calibrator is not perfect, due to vibration, as addressed in section 2.2.4. The idea of approximating the thermal behavior of the dihedral mirrors, collimator, and detectors with Planck functions, as Fixsen describes [38], does not rest on solid grounds. Each material should ideally have been measured in the laboratory, as real materials do not behave as blackbody sources [80]. For instance, the FIRAS team describes harmonic responses in the instrument when radiation passes through the system more than once. This proves that the interior components of the instrument cannot be modeled as perfect blackbodies. They do provide reflective surfaces. It is noted that $\sim$20% of the input signal fails to reach the output [38]. This is a large number, which represents frequency dependent losses. However, no frequency dependence is mentioned, presumably because the loss for each interferogram cannot be dissected in these terms. Both second and third order harmonics were thought to be significant at the 0.1% level [38]. They also report that the frequency scale for FIRAS does not quite agree with that determined using known spectral lines. In order to correct the situation, they make a 0.5% adjustment with "*the remainder being absorbed by a 4 mK adjustment in the absolute temperature scale*" [38].

The discussion relative to the bolometers highlights how modeling can misrepresent the actual behavior of a device. The FIRAS team writes: "*The total of nine parameters with their uncertainties and covariance matrix were determined*

from these tests. The agreement with the determination of the parameters from the FIRAS in-orbit calibration is poor, with normalized χ^2's of 80 to 800 in various fits for 9 DOF (degrees of freedom). This is probably due to a deficit in the bolometer model" [38]. In the final analysis, the in-flight calibration procedure is viewed as correct, and the disagreement with pre-flight data appears to be disregarded. This demonstrates how the COBE calibration procedures have become essentially detached from any experimental findings recorded on the ground before flight.

The calibration process brings many more degrees of freedom for setting error bars and temperatures. Mather et al. thus write: "*However, the calibration process corrects other effects of the error to the first order...*" [42]. Calibration involves: "*comparison of the sky with an ideal movable external blackbody calibrator (Xcal) that can fill the aperture of the sky horn. The rest of the calibration process is used to measure gains and offsets that apply if the calibrator spectrum does not match the sky spectrum*" [43]. As a result, the FIRAS team can achieve a perfect fit to the sky spectrum. They have sufficient degrees of freedom to accomplish the task by invoking the calibration procedure. The inversion matrix required for the calibration fits is "*of such large rank (∼4,000)*" that it "*is not generally tractable*" [38]. The FIRAS team was "*able to invert this matrix by taking advantage of its special form... This made inversion possible, though still not speedy*" [38].

Relative to error analysis, very large degrees of freedom (DOF) were invoked. The FIRAS team writes: "*The normalized χ^2 resulting from this fit is 2.8218 (27873 DOF) for the left low detector, short slow stroke data ($2.27 < \nu < 21.54$ cm^{-1}), and 4.53 for (159353 DOF) for the right high detector, short slow stroke data ($2.27 < \nu < 96.28$ cm^{-1})*" [38]. Moreover, it can be deduced that the values are rather high for χ^2/DOF, particularly when operating away from the null position. Cheng [34] reports higher than expected χ^2/DOF values, of 4 to 10, for the low and high frequency channels when discussing the calibration data. Apparently [34], it is only when considering calibration files near the null condition that χ^2/DOF values near 1 are reached [39]. Of course, it is easier to fit data near the null, for the precise reason that the spectrum contains little power in this range. It is solely by examining the performance of the calibration model away from the null, that any real insight can be harnessed relative to the reliability of this method. However, such data appears to give even higher χ^2/DOF values than obtained near the null [34]. This is not a good sign, relative to the validity of this approach. The inability to find good χ^2/DOF values off the null might be reflecting leakage around Xcal, for instance. This could become more apparent when Xcal and Ical are at very different temperatures.

Fixsen et al. [39] do describe excellent χ^2/DOF performance in their Figure 1 (not reproduced herein). An analysis of Table 1 in [39] reveals that χ^2/DOF are generally on the order of 2 or more. Nonetheless, it is noticeable that the χ^2/DOF, listed in this work (see Table 1 in [39]), have improved substantially over those found 2 years earlier (see Table 2 in [38]). It is not clear if this represents anything but better insight into how χ^2/DOF values could be minimized. In the end, there is too much flexibility in these approaches. This places at risk all physically meaningful experimental findings, reflecting systematic errors.

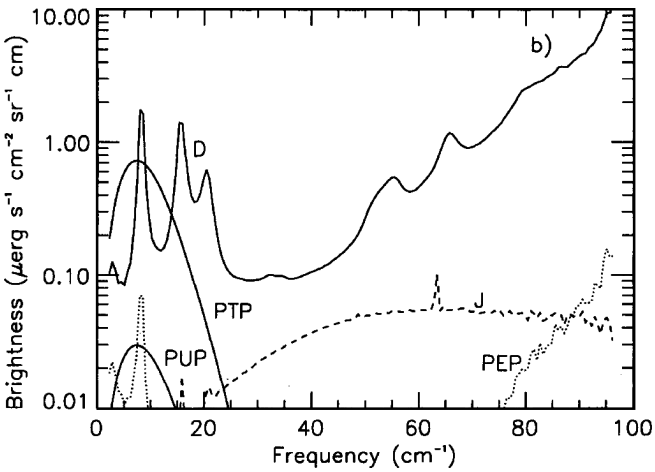

Fig. 10: Plot of various error terms for the FIRAS high frequency channel for a typical sky point, as reproduced from [38]. Separate fits are obtained for each point in the sky. This allows for far too many degrees of freedom in the FIRAS calibration stage. Curve D represents the error arising from detector sensitivity. Note the resonances at ∼7, 16, and 20 cm^{-1}. These may correspond to CO lines in the galaxy. Such resonances should not be found on functions representing detector sensitivity. They are not found in the detector functions at low frequency [38]. The dashed line, which is not labeled in the original work, represents the calculated errors from the galaxy as can be established using Figure 13. Note that there is little error contribution from the galaxy, below 20 cm^{-1}. As such, the FIRAS team cannot attribute the failure to achieve a proper null to the presence of contaminating galactic signal in this frequency region. The dotted line, PEP, accounts for error associated with various temperatures within the instrument. Once again, a resonance line is observed at ∼7 cm^{-1}. Such a resonance line should not be found on this function. It would, however, permit the FIRAS team to vary the error in this region when trying to correct for contributions from galactic CO. PTP accounts for errors in the absolute temperature scale. PUP error depends on the absolute temperature state of the instrument and is most sensitive to Ical. PUP and PTP are given a blackbody appearance without proper justification by the FIRAS team (see text for additional details). Reproduced by permission of the AAS.

A treatment by Fixsen et al. [38] of the error terms for FIRAS reveals that the FIRAS team considered nearly every possible source of instrumental contribution, while discounting the possibility that errors existed in the shape of the blackbody provided by the sky itself. Such a systematic error could exist if diffraction effects were important.

Figure 10 is a reproduction of Figure 9b in [38]. For

the low frequency channel (figure not displayed), the major term is referred to as PTP. It represents the uncertainty in the absolute temperature scale. The peak brightness of a 2.7 K blackbody is approximately 120 μergs cm^{-2} s^{-1} sr^{-1} cm [38]. As a result, this error term absorbs about 0.5% of the deviation from the peak of a blackbody. The most important error term for the high frequency channel, D, accounts for detector noise. The PUP error is linked to the temperature state of the instrument and is primarily dependent on Ical. The PEP error depends on the temperatures of various emitters in the instrument. "*These are: Ical 2.76±0.006 K, MTM 2.0±0.4 K, horns 2.75±0.005 K, mirrors 1.56±0.02 K, and bolometers 1.52±0.017 K*" [38]. The FIRAS team writes that the PEP and PUP error terms are well approximated by Planckian functions. This claim, however, is without foundation. In fact, there are no references provided for assigning a Planckian shape [10] to either PTP or PUP. Assigning such shapes to these two terms will help determine the appearance of the other terms. The entire procedure is without scientific basis [80]. It is particularly concerning that the FIRAS team generates such error functions for each point in the sky. Instrument error should not be dependent on the scan direction. At the same time, it is true that the instrument experiences temperature fluctuations over time: "*Further tests of the calibration are obtained by searching the calibrated map of the sky for features relating to changes of the instrument state. The largest such changes occurred during the time from 1990 May to August. In this time period, it was impossible to keep both the Earth and the Sun below the Sun screen, and the Earth illuminated the top of the instrument during part of the orbit. The data taken with the Earth above the instrument were rejected in the maps, but the thermal transient produced by the heat of the Earth was large and long. As a result, we raised the set point of the horn temperature controllers to as high as 6 K to achieve stability*" [38]. Direct visualization of the Earth did impact the COBE results, but the data were rejected. Yet, if the Earth was truly silent over the frequency of interest, there could be no reason to reject this data. Heating by the Earth could simply be accounted for in a manner similar to that used for other parts of the orbit. The FIRAS team believes that the heat transient in the instrument, as a consequence of direct infrared heating, was the only effect. However, it would have been most interesting to examine the resulting sky interferograms. Perhaps these actually contained direct physical proof that the Earth had emitted the microwave background.

In any case, note the nature of the error term, D, for the high frequency channels. Essentially, there are resonance lines at ∼7, ∼16, and ∼20 cm^{-1}. These features seem to correspond to the presence of the CO lines in the galaxy [39]. Such lines should not be found within detector noise error. In addition, curve D for the high frequency channels approaches 10 μergs cm^{-2} s^{-1} sr^{-1} cm, at 95 cm^{-1}. This is an extremely powerful contribution from this term, given that the maximal power of the microwave background itself is on the order of 120 μergs cm^{-2} s^{-1} sr^{-1} cm.

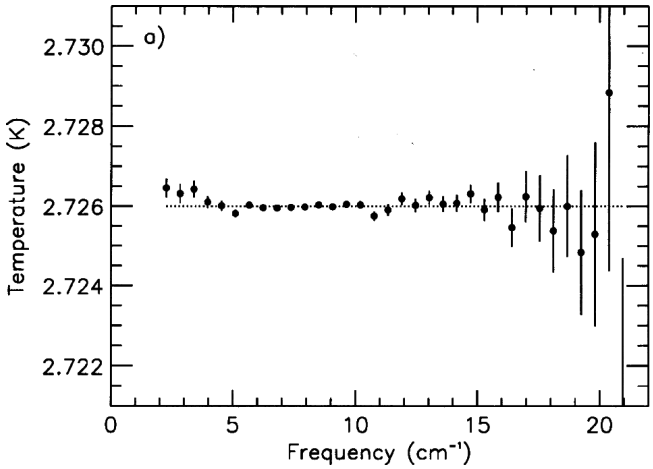

Fig. 11: Calculated residual errors in the microwave background, as reproduced from [35]. These residuals were generated, using a conservative approach, by increasing the statistical errors, forcing χ^2 to 32 [35]. Nonetheless, note the systematic increase in the residuals beyond 15 cm^{-1}. There is a slight trend towards signal loss in this region as well. In addition, the points below 5 cm^{-1}, slowly begin to rise away from the reported temperature, and represent signs of excessive signal in this region of the spectrum. The residuals are presented once again in 2001 [44]. At this time, systematic variations have been absorbed by the calibration files and the residuals are now random and of insignificant importance. Reproduced by permission of the AAS.

2.4.2 Analysis of residual errors

When Mather et al. [35] publish the 1994 FIRAS data release, several unexpected findings are revealed. Figure 1 of this work [35], a presentation of the CMBR residuals, is reproduced as Figure 11. There are two interesting aspects of this figure. First, there is a pronounced increase in the error bars associated with the residuals, as the frequencies are raised beyond 15 cm^{-1}. This increase in variability is systematic, and consequently may represent a real finding. In fact, there is a slight trend towards decreased temperatures as a function of frequency beyond 15 cm^{-1}. Second, at the lower frequencies, the data points begin to rise. The FIRAS team comments as follows: "*pending further detailed study of possible instrument faults at these low frequencies, we cannot speculate on their nature. We emphasize that the size of the apparent deviations is greatest at those frequencies where diffractive effects, interferogram baseline curvature, and very low spectral resolving power and wide spectral sidebands cause the greatest difficulties in calibration*" [35]. The authors therefore "*conservatively increase the statistical errors by a factor, forcing χ^2 to exactly 32, the number of degrees of freedom in the fit*" [35]. Nonetheless, they eventually publish

new residuals [44], which have now lost the systematic variations displayed in Figure 11. This shows the power of the fitting methods applied.

The FIRAS team believes that they fully understand all systematic errors and that their fits are justified. However, this is not the case. The fact that an excellent fit can be found, given sufficient degrees of freedom, is well recognized in science. The question remains how well justified were the bases for the fits. Adequate justification is based on a complete understanding of the instrument on the ground with calibrated test procedures. This approach was not utilized. Instead, fits are obtained by adjusting gains, offsets, and functions, which have a weak foundation, other than their ability to result in minimal residual errors for the sky. Furthermore, the FIRAS team has not shown that it can minimize residuals, using their final calibrations across all ranges of temperatures for Xcal, Ical, the sky horn, and the reference horn. Without explicit demonstration that the final calibrations apply to all possible interferograms, the analysis of residuals for the sky alone have little value. It is a complement of all residuals, for all conditions, which is important to visualize, for this alone might help establish the reliability of the approach in the absence of sufficient pre-flight testing.

2.4.3 Data omission

The FIRAS data set from 1994 contains a more serious concern: all of the observations at frequencies below 2 cm^{-1} are now excluded [35]. Moreover, there is a rise in the residuals below 4 cm^{-1} which cannot be accounted for by their error bars. This region is usually the easiest to monitor due to the low frequency range. Never again is the data below 2 cm^{-1} re-included in the FIRAS data set. It is only through reading the accompanying calibration work by Fixsen et al. [38], that one might postulate on the causes behind the loss of this data. A single sentence is presented when discussing the reference horn: "*However, the measured emission is higher than predicted, particularly at the lowest frequencies*" [38].

Though FIRAS was designed to cover the region from 1–2 cm^{-1}, the FIRAS team omits the data below 2 cm^{-1} and ignores the excessive signal. They do not discuss the cause of this anomaly, unless Wilkinson's concerns about earthshine were a reaction to this problem [74]. At the same time, given the use of calibration files to correct FIRAS, it may have been that the FIRAS team could not envision a means to account for the spectral behavior below 2 cm^{-1}. On the surface, ignoring this data might not appear so serious. After all, the entire spectrum beyond 2 cm^{-1} was reported.

Given that diffraction of a terrestrial signal would produce distortions in the measurement of the microwave background, which include excessive signal at low frequencies and decreased signal as frequencies increase, the dismissal of this data cannot be taken lightly. The FIRAS team also forsakes all data acquired when the Earth was directly illuminating FIRAS [38], as previously discussed in section 2.4.1. While infrared heating of the instrument did occur at this time, it is not evident that such heating could not be modeled. This is the type of evidence that may have pointed to an earthly source for the microwave background.

2.4.4 Error bars

Despite the presence of systematic errors, the FIRAS team is able to essentially sidestep the recordings of their thermometers and overcome their inaccuracy. E. S. Cheng summarizes the overall approach of the group: "*Since the FIRAS is a far more sensitive thermometer that the GRT's (germanium resistance thermometers), especially at temperatures above 3 K, the thermometer readings can be adjusted, using the calibration data, to provide maximal internal consistency and a refined temperature calibration*" [34]. As such, the readings of the physical thermometers could be given less weight.

Initially, it is not evident if they are aware that errors in the thermometers limit the ultimate temperature that can be reported for the microwave background. In 1996, Fixsen et al. arrive at a microwave background temperature of 2.730 ± 0.001 K (see Table 1), which relies on Xcal (see page 581, section 4.1, in [39]). Then, three years later, in 1999, the FIRAS team writes: "*A 5 mK error in the temperature determination of Xcal leads directly to a 5 mK error in the temperature determination of the CMBR*" [42]. The team apparently realized that it was impossible for Fixsen et al. [39] to claim a 1 mK error bar for this measurement in 1996. But, they continue to discount the 18 mK error between the Ical thermometers [38].

In order to fully restrict the error bars on the determination of the microwave background, the COBE group therefore moves to adopt two additional methods which, at least on the surface, are independent of Xcal. In the first instance, they determine the temperature by calibrating the frequencies of the background, using lines from CO and C+ [39]. Few details are provided relative to this approach; however, it may rely on accurately defining a Wien maximum and extracting the temperature from Wien's law [11]. The method is solid, on the surface at least. Nonetheless, it will depend on correctly setting the peak in the microwave background data, which may in turn depend on Ical and/or Xcal. The ability to detect a proper Wien maximum [11] would also be sensitive to interference effects caused by diffraction on the COBE shield, should the signal originate from the Earth. As a result, it is not clear that the frequency method holds any less systematic error than that directly relying on Xcal.

Alternatively, the group also uses the existence of a dipole to extract a monopole temperature [39]. In this way, they can build on the findings of the DMR relative to the dipole value [46–49]. Once again, the method may appear more accurate, but is also subject to many of the same problems as that based on Xcal. If the use of frequency calibration, or of

the dipole, seems less prone to systematic error, it may simply be because these have escaped detection by the FIRAS team. It is well established, not only in physics, but across the sciences, that systematic errors can be extremely difficult, even impossible, to detect [88]. Consequently, one must not dismiss those systematic errors which are evident.

Using a combination of these three methods, the FIRAS team finally arrives at a microwave background temperature of 2.725±.00065 K [43]. Beyond undetected systematic errors, this number circumvents much of the planning built into Xcal and Ical. It also neglects the excessive signal detected below 2 cm^{-1}. Relative to error bars, the result obtained, using an average of many methods, was analogous to ignoring the existence of known temperature error in the reference calibrators Xcal and Ical. The existence of imperfect nulls was also dismissed, as were all interferograms obtained while the Earth was directly illuminating FIRAS.

In the absence of proper pre-flight testing, it is impossible to account, with certainty, for all possible source of systematic errors associated with inability to find a null. Data processing methods do not address the fundamental issue. The FIRAS team believes that it has fully understood all systematic errors and that they can be removed from the final error report. But, systematic errors are best treated through the proper design and testing of scientific instruments on the ground. This was not achieved. The calibration procedure creates the illusion that all systematic error can be taken into account, after completion of data acquisition. This is not a prudent approach to systematic error, especially since they can be nearly impossible to identify [88, p. 93–95]. It is best to report all known systematic errors within the final error bar.

In failing to achieve a clear null, FIRAS is pointing to something on the order of a 34 mK error. The overall error in Xcal was ∼5 mK. The error difference between the Ical thermometers is 18 mK and the drift for Ical is 3 mK. A frequency correction of ∼4 mK exists. Some of these errors may be related and could be added quadratically [88, p. 93–95]. Direct addition provides a worse case scenario of ∼64 mK [88, p. 93–95]. As such, using direct addition, ∼64 mK appears to be a good lower limit on the accuracy of the FIRAS data set, from 2–20 cm^{-1}. This treatment would discount attempts to lower the error bar to 1 mK in the final FIRAS report [43]. In fact, ∼64 mK is not far from the 60 mK error initially used by the FIRAS team [32]. At the same time, the group asserts that their data is "*indistinguishable from a blackbody*" [37]. A cursory examination would suggest that this was the case (see Figure 2). An understanding of calibration process has provided the explanation.

2.4.5 The optical transfer function

The FIRAS team first presents the optical transfer function in the Explanatory Supplement, in 1997 [40]. This function is critical in processing FIRAS data files [40, p. 50] and it is reproduced herein as Figure 12. For an ideal spectrometer, the optical transfer function would be unity over the entire frequency range. That is, for every photon which enters the system, one photon is recorded by the detector. This situation does not occur in practice, and transfer functions will deviate from ideality. But, the transfer function for FIRAS is much less than ideal. At the lowest frequencies (<20 cm^{-1}), the transfer function contains a very strange and unexplained oscillation. The FIRAS team does not comment on the cause of this feature. Nonetheless, since the reciprocal of the transfer function is used to process data, this oscillation is significant. Although difficult to ascertain, this feature might be a sign of signal diffraction into the horn. In any event, the discontinuity near 20 cm^{-1} is due to the filter cutoff between the low and high frequency channels.

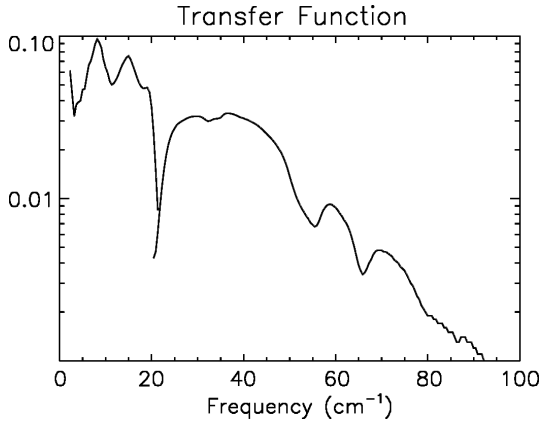

Fig. 12: Illustration of the Optical Transfer Function for FIRAS, as reproduced from the Explanatory Supplement [40]. The features near 20 cm^{-1} are due to the position of the filter cutoff. Nonetheless, this does act to provide a substantial correction for signal beyond the Wien maximum and between 15 and 20 cm^{-1}. Note the oscillation present below this frequency range. It is not clear why such features should be present on this optical transfer function. These might represent the effect of constructive and destructive interference. It is impossible to truly ascertain their cause with the data provided. Most importantly, the optical transfer function is decreasing exponentially. This is not characteristic of a properly functioning spectrophotometer. This figure reveals that the FIRAS instrument is suboptimal, beyond ∼30 cm^{-1}. Reprinted with permission of John Mather.

The most noteworthy feature of the optical transfer function for FIRAS is that only 1 photon in 10 is being detected, at best. In addition, the plot is on a logarithmic scale. Such behavior is highly unusual and demonstrates that the FIRAS instrument is not linear. It is also not sensitive at the higher frequencies. As a result, when the optical transfer function is applied to process data beyond 30 cm^{-1}, it results in a pronounced amplification of spectral noise. This is revealed in Figure 13 [41], where noise in the fits is amplified beyond 40 cm^{-1}. This constitutes a solid illustration that the FIRAS instrument, for practical purposes, is subfunctional in this frequency range.

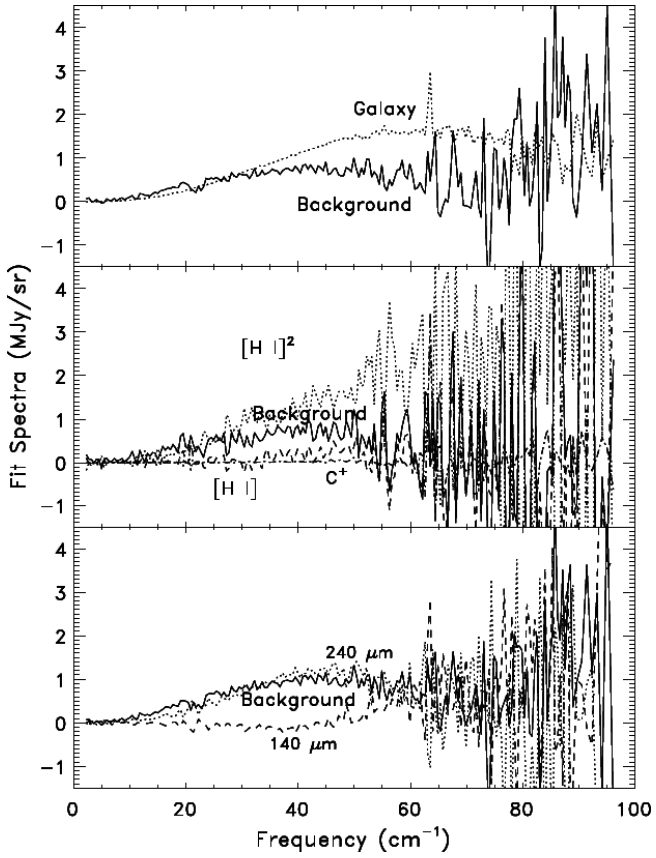

Fig. 13: Fit spectra calculated across the high frequency region using the FIRAS instrument, as reproduced from [41]. Note the tremendous increase in random errors beyond 30 cm^{-1}. This indicates that the spectrometer is suboptimal, in this frequency range. Reproduced by permission of the AAS.

2.4.6 Comments made by other authors

Several Italian authors [89–91] have been interested in the calibration of the FIRAS instrument as Fixsen and Mather highlight [42]. Giorgi, for instance, suggests that there could be an asymmetry of as much as 5% in the two input arms of FIRAS [89]. Fixsen and Mather point out that the measured asymmetry is only 1–3% [42]. In defending FIRAS data, Fixsen and Mather write: "*However, one must also consider the source of any reflection. The Xcal is part of a closed cavity composed of the calibrator, the sky horn, a small gap between the calibrator and the sky, and a small aperture leading to the spectrometer horn. Consequently, the radiation reflected by the calibrator must have originated either from itself, the sky horn, the sky through the gap, or the small aperture to the spectrometer. Three of these sources are effectively at the temperature of the CMB. As the most emissive of the four, the source of most of the reflected radiation is the calibrator itself... Moreover, since both the horn and the Xcal temperatures were set to match the CMB temperature, the only source of radiation that could be reflected by the calibrator and that was not at the CMB temperature is the small aperture leading to the spectrometer*" [42]. Such a statement cannot be justified. It is not clear that the sky is at the temperature of the CMB. Should the signal originate from the Earth, it would undergo differential diffraction as a function of frequency, as it travels over the RF shield and into the horn. This would lead to a spectrum which is not blackbody, and the measured sky spectrum would not be at the exact temperature of the microwave background. It would be distorted. Fixsen and Mather cannot assume that the sky is a blackbody at the temperature of the CMB. That is what they are trying to determine.

Work by Battistelli et al. [90] is centered on a computational analysis of Xcal, in order to further refine cosmological parameters. The text does not constitute a criticism of FIRAS. The emissivity values obtained for Xcal, are nearly ideal. Salvaterra and Burigana [91] examine a range of issues in detail, but the text does not raise any real concerns relative to FIRAS.

3 The Differential Microwave Radiometers (DMR)

The COBE satellite is also equipped with Differential Microwave Radiometers, the DMR. These constitute three pairs of narrow band antennae operating at 31.5, 53, and 90 GHz [46]. The DMR are mounted directly on the sides of the helium dewar containing the FIRAS and DIRBE instruments [45]. A detailed treatment of the DMR will not be presented, as many of the issues relative to the DMR have already been addressed relative to the WMAP satellite [20]. It is clear that the DMR has measured a dipole. This result is highly significant.

Of all the concerns which the DMR shares with WMAP, the central issue remains the processing of data and the extraction of the multipoles [20]. These are the "*wrinkles on the fabric of time*" [21]. Before the multipoles can be analyzed, the signal from both the dipole and galactic foreground must be removed. Importantly, as Smoot discusses in his popular book [21], these investigators also remove the quadrupole signal from the underlying maps. It is only at this stage that the multipoles become visible. Smoot writes: "*We were confident that the quadrupole was a real cosmic signal... By late January and early February, the results were beginning to gel, but they still did not quite make sense. I tried all kinds of different approaches, plotting data in every format I could think of, including upside down and backwards, just to try a new perspective and hoping for a breakthrough. Then I thought, why not throw out the quadrupole — the thing I'd been searching for all those years — and see if nature had put anything else there!*" [21, 276–277]. After removing the quadrupole, the multipoles finally appeared. Smoot then comments [21, 279]: "*Why, I puzzled, did I have to remove the quadrupole to see the wrinkles?*"

The answer to this question is one of data processing.

The raw maps do not contain any systematic signal variations on their own [21, 276–279]. The signals were random in nature. However, when Smoot and his colleagues imposed a systematic removal of signal, they produced a systematic remnant. In essence, the act of removing the quadrupole created the multipoles and the associated systematic anisotropy. Once the quadrupole was removed, the multipoles appeared as extremely consistent variations on the maps. As previously mentioned, these findings have no relevance to cosmology and are purely an artifact of signal processing. Citing from previous work [20]: "*Apparent anisotropy must not be generated by processing*". The sky does have anisotropy. But this anisotropy is likely to remain random, as Smoot initially observed in his data set, before removal of the quadrupole.

4 Conclusion

Through this analysis, unexpected problems with FIRAS and the DMR data have been brought to light. With regard to FIRAS, many issues exist. They include: 1) lack of gain and side lobe characterization for the FIRAS horn, 2) absence of diffraction modeling involving the interaction between FIRAS and the shield, 3) rudimentary pre-flight testing, 4) failure to document side lobe performance, in space, at frequencies relevant to the microwave background, 5) inappropriate evaluation of Xcal emissivities, 6) inability to ensure that leakage did not occur around Xcal in flight, given the vibrations present, the lack of gravity, and the nature of the Kapton leaves, 7) existence of a suboptimal transfer function for the instrument, 8) the presence of systematic errors, for the Xcal and Ical thermometers, 9) inability to achieve a proper null between the sky and Ical, 10) inability to reach a proper null between Xcal and Ical, 11) excessive degrees of freedom during the calibration process, 12) lack of justification for the error functions PTP and PUP, 13) inappropriate minimization of error bars, 14) omission of data below 2 cm^{-1} from all final data releases, and 15) omission of data when the Earth was directly illuminating FIRAS.

Given the systematic errors on Xcal, Ical, the frequency drift, and the null temperature, it is reasonable to ascertain that the FIRAS microwave background temperature has a significant error bar. As such, an error on the order of 64 mK represents a best case scenario, especially in light of the dismissal/lack of data at low frequency. The report of a microwave temperature of 2.725 ± 0.001 K [43] does not accurately reflect the extent of the problems with the FIRAS instrument. Furthermore, the absolute temperature of the microwave background will end up being higher than 2.725 K, when measured without the effect of diffraction, and when data below 2 cm^{-1} is included. Contrary to popular belief, the FIRAS instrument did not record the most perfect blackbody spectrum in the history of science.

Relative to the DMR, the problems mirror, to a large extent, those I voiced earlier with WMAP [20]. The most pressing questions are centered on the ability to remove the quadrupole from the maps of the sky. In so doing, it is clear that a systematic residual will be created, which can easily be confounded for true multipoles. In the end, the methods to process the anisotropy maps are likely to be "creating anisotropy" where none previously existed.

It also remains fascinating that the astrophysical community has not expressed greater anxiety relative to the difficulties produced by water, in the lower atmosphere. This is perhaps the most serious area of concern. It is certainly true that the Earth is bathed in a field with an apparent temperature near 3 K. The existence of the dipole is also firmly established. Cosmology holds that the monopole signal [1] represents a remnant of creation. Conversely, I maintain, along with my colleagues [5, 7], that it is being produced by the oceans of the Earth. Through this work, it is my hope that others will begin to see that there are legitimate issues with the FIRAS and DMR results on COBE. The thermal emission of water, in the microwave and far infrared, remains incompletely characterized. Our planet has never been eliminated as the source of the microwave background. In the end, the PLANCK satellite [86] should reveal that the Penzias and Wilson monopole [1] was never present in the depth of the Cosmos. The signal belongs to the Earth.

Acknowledgement

John Mather is recognized for granting permission to reproduce figures on behalf of the COBE team.

Dedication

This work is dedicated to Professor A. J. Christoforidis for the faith he demonstrated relative to my work these many years and for conferring upon me the privilege of becoming a professor of radiology.

Submitted on June 24, 2009 / Accepted on July 03, 2009
First published online on July 16, 2009

References

1. Penzias A.A. and Wilson R.W. A measurement of excess antenna temperature at 4080 Mc/s. *Astrophys. J.*, 1965, v. 1, 419–421.
2. Dicke R.H., Peebles P.J.E., Roll P.G., and Wilkinson D.T. Cosmic black-body radiation. *Astrophys. J.*, 1965, v. 1, 414–419.
3. Robitaille P.-M.L. A radically different point of view on the CMB. In: *Questions of Modern Cosmology — Galileo's Legacy*, ed. by M. D'Onofrio and C. Burigana, Springer, New York, N.Y., 2009.
4. Robitaille P.M.L. The Earth microwave background (EMB), atmospheric scattering and the generation of isotropy. *Prog. in Phys.*, 2008, v. 2, L7–L8.

5. Rabounski D. The relativistic effect of the deviation between the CMB temperatures obtained by the COBE satellite. *Prog. in Phys.*, 2007, v. 1, 24–26.
6. Robitaille P.M.L. Water, hydrogen bonding, and the microwave background. *Prog. in Phys.*, 2009, v. 2, L5–L7.
7. Rabounski D. and Borissova L. On the earthly origin of the Penzias-Wilson microwave background. *Prog. in Phys.*, 2009, v. 2, L1–L4.
8. Stewart B. An account of some experiments on radiant heat, involving an extension of Prévost's theory of exchanges. *Trans. Royal Soc. Edinburgh*, 1858, v. 22(1), 1–20 (also found in Harper's Scientific Memoirs, edited by J. S. Ames: The Laws of Radiation and Absorption: Memoirs of Prévost, Stewart, Kirchhoff, and Kirchhoff and Bunsen, translated and edited by D. B. Brace, American Book Company, New York, 1901, 21–50).
9. Kirchhoff G. Über das Verhältnis zwischen dem Emissionsvermögen und dem Absorptionsvermögen. der Körper für Wärme und Licht. Poggendorfs Annalen der Physik und Chemie, 1860, v. 109, 275–301 (English translation by F. Guthrie: Kirchhoff G. On the relation between the radiating and the absorbing powers of different bodies for light and heat. *Phil. Mag.*, 1860, ser. 4, v. 20, 1–21).
10. Planck M. Über das Gesetz der Energieverteilung im Normalspektrum. *Annalen der Physik*, 1901, v. 4, 553–563 (English translation by ter Haar D.: Planck M. On the theory of the energy distribution law in the normal spectrum. The old quantum theory. Pergamon Press, 1967, 82–90; also Planck's December 14, 1900 lecture *Zur Theorie des Gesetzes der Energieverteilung in Normalspectrum*, which stems from this paper, can be found in either German, or English, in: Kangro H. Classic papers in physics: Planck's original papers in quantum physics. Taylor & Francis, London, 1972, 6–14 or 38–45).
11. Wien W. Über die Energieverteilung in Emissionspektrum eines schwarzen Körpers. *Ann. Phys.*, 1896, v. 58, 662–669.
12. Stefan J. Über die Beziehung zwischen der Warmestrahlung und der Temperature. *Sitzungsberichte der mathematischnaturwissenschaftlichen Classe der kaiserlichen Akademie der Wissenschaften Wien*, 1879, v. 79, 391–428.
13. Robitaille P.M.L. On the validity of Kirchhoff's law of thermal emission. *IEEE Trans. Plasma Sci.*, 2003, v. 31(6), 1263–1267.
14. Robitaille P.M.L. An analysis of universality in blackbody radiation. *Prog. in Phys.*, 2006, v. 2, 22–23; arXiv: physics/0507007.
15. Robitaille P.M.L. Blackbody radiation and the carbon particle. *Prog. in Phys.*, 2008, v. 3, 36–55.
16. Robitaille P.M.L. A critical analysis of universality and Kirchhoff's law: a return to Stewart's law of thermal emission. *Prog. in Phys.*, 2008, v. 3, 30–35; arXiv: 0805.1625.
17. Robitaille P.M.L. Kirchhoff's law of thermal emission: 150 years. *Prog. in Phys.*, 2009, v. 4, 3–13.
18. COBE website, http://lambda.gsfc.nasa.gov/product/cobe
19. WMAP website, http://map.gsfc.nasa.gov
20. Robitaille P.-M.L. WMAP: A radiological analysis. *Prog. in Phys.*, 2007, v. 1, 3–18.
21. Smoot G. and Davidson K. Wrinkles in time: witness to the birth of the Universe. Harper Perennial, New York, N.Y., 1993.
22. Mather J.C. and Boslough J. The very first light. Basic Books, New York, N.Y., 1996.
23. Mather J.C. COBE-explorer of the primeval explosion. *Astronautics & Aeronautics*, 1978, v. 16, 60–66.
24. NASA. Redesign of the Cosmic Background Explorer (COBE), Academy of Program/Project & Engineering Leadership (available online through NASA).
25. Mather J.C., Toral M., Hemmati H. Heat trap with flare as multimode antenna. *Appl. Optics*, 1986, v. 25(16), 2826–2830.
26. Milan L.J. Test facility requirements for the thermal vacuum thermal balance test of the cosmic background explorer. *Journal IES*, 1991, March/April, 27–33.
27. Mosier C.L. Thermal design of the cosmic background explorer cryogenic optical assembly. *AIAA*, *Aerospace Sciences Meeting*, 29th, Reno, NV, Jan. 7–10, 1991, 1–6.
28. Coladonato R.J., Irish S.M, and Mosier C.L. Cryogenic Optical Assembly (COA) cooldown analysis for the Cosmic Background Explorer (COBE). *Third Air Force/NASA Symposium on Recent Advances in Multidisciplinary Analysis and Optimization*, 1990, 370–377.
29. Hagopian J.G. FIRAS optical alignment and performance during vibration qualification and cryogenic cycling. *Cryogenic Optical Systems and Instruments III*: Proceedings of the SPIE, 1989, v. 973, 117–131.
30. Barney R.D. and Magner T.J. FIRAS wire grid characterization techniques. *Cryogenic Optical Systems and Instruments III*: Proceedings of the SPIE, 1989, v. 973, 139–146.
31. Serlemitos A.T. Flight worthy infrared bolometers with high throughput and low NEP. *Cryogenic and Optical Systems III*: *Proceedings of the SPIE*, 1989, v. 973, 314–321.
32. Mather J.C., Cheng E.S., Eplee R.E., Isaacman R.B., Meyer S.S., Shafer R.A., Weiss R., Wright E.L., Bennett C.L., Boggess N., Dwek E., Gulkis S., Hauser M.G., Janssen M., Kelsall T., Lubin P.M., Moseley S.H., Murdock T.L., Silverberg R.F., Smoot G.F., and Wilkinson D.T. A preliminary measurement of the cosmic microwave background spectrum by the cosmic background explorer (COBE) satellite. *Astrophys. J.*, 1990, v. 354, L37–L40.
33. Mather J.C., Fixsen D.J., and Shafer R.A. Design for the COBE Far Infrared Absolute Spectrophotometer (FIRAS). *Proc. SPIE*, 1993, v. 2019, 168–179; http://lambda.gsfc.nasa.gov/data/cobe/firas/doc/FES4_APP_B.PS
34. Cheng E.S. Far-infrared cosmology measurements — the FIRAS spectrum and other curious results. *Astronomical Soc. Pac. Conf. Ser. Observational Cosmology*, 1993, v. 51, 501–511.
35. Mather J.C., Cheng E.S., Cottingham D.A., Eplee R.E., Fixsen D.J., Hewagama T., Isaacman R.B, Jensen K.A., Meyer S.S., Noerdlinger P.D., Read S.M., Rosen L.P., Shafer R.A., Wright E.L., Bennett C.L., Boggess N.W., Hauser M.G., Kelsall T., Moseley S.H., Silverberg R.F., Smoot G.F., Weiss R, and Wilkinson D.T. Measurement of the cosmic microwave background spectrum by the COBE FIRAS Instrument. *Astrophys. J.*, 1994, v. 420, 439–444.

36. Fixsen D.J.,Cheng E.S., Cottingham D.A., Eplee R.E., Isaacman R.B., Mather J.C., Meyer S.S., Noerdlinger P.D., Shafer R.A., Weiss R., Wright E.L., Bennett C.L., Boggess N.W., Kelsall T., Moseley S.H., Silverberg R.F., Smoot G.F., and Wilkinson D.T. Cosmic microwave background dipole spectrum measured by COBE FIRAS. *Astrophys. J.*, 1994, v. 420, 445–449.
37. Wright E.L., Mather J.C., Fixsen D.J., Kogut A., Shafer R.A., Bennett C.L., Boggess N.W., Cheng E.S., Silverberg R.F., Smoot G.F., and Weiss R. Interpretation of the COBE FIRAS CMBR spectrum. *Astrophys. J.*, 1994, v. 420, 450–456.
38. Fixsen D.J., Cheng E.S., Cottingham D.A., Eplee R.E., Hewagama T., Isaacman R.B, Jensen K.A., Mather J.C., Massa D.L., Meyer S.S., Noerdlinger D.P., Read S.M., Rosen L.P., Shafer R.A., Trenholme A.R., Weiss R., Bennett C.L., Boggess N.W., Wilkinson D.T., and Wright E.L. Calibration of the COBE FIRAS instrument. *Astrophys. J.*, 1994, v. 420, 457–473.
39. Fixsen D.J., Cheng E.S., Gales J.M, Mather J.C., and Shafer R.A., and Wright E.L. The cosmic microwave background spectrum from the full COBE FIRAS data set. *Astrophys. J.*, 1996, v. 473, 576–587.
40. Brodd S., Fixsen D.J., Jensen K.A., Mather J.C., and Shafer R.A. Cosmic background explorer (COBE) Far Infrared Absolute Spectrophotometer (FIRAS) Explanatory Supplement. NASA, 1997; lambda.gsfc.nasa.gov/data/cobe/firas/doc/FES4_ABSPREF.PS
41. Fixsen D.J., Dwek E., Mather J.C., Bennett C.L., Shafer R.A. The spectrum of the extragalactic far-infrared background from the COBE FIRAS observations. *Astrophys. J.*, 1998, v. 508, 123–128.
42. Mather J.C., Fixsen D.J., Shafer R.A., Mosier C., and Wilkinson D.T. Calibrator design for the COBE far infrared absolute spectrometer (FIRAS). *Astrophys. J.*, 1999, v. 512, 511–520.
43. Fixsen D.J. and Mather J.C. The spectral results of the far-infrared absolute spectrophotometer instrument on COBE. *Astrophys. J.*, 2002, v. 581, 817–822.
44. Wright E. Cosmic microwave background. Encyclopedia of Astronomy and Astrophysics (Paul Murdin, Ed.), Institute of Physics Publishing, Bristol, U.K., 2001, v. 1, 524–530.
45. Boggess N.W., Mather J.C., Weiss R., Bennett C.L., Cheng E.S., Dwek E., Gulkis S., Hauser M.G., Janssen M.A., Kelsall T., Meyer S.S., Moseley S.H., Murdock T.L., Shafer R.A., Silverberg R.F., Smoot G.F., Wilkinson D.T., and Wright E.L. The COBE mission: its design and performance two years after launch. *Astrophys. J.*, 1992, v. 397, 420–429.
46. Smoot G., Bennett C., Weber R., Maruschak J., Ratliff R., Janssen M., Chitwood J., Hilliard L., Lecha M., Mills R., Patschke R., Richards C., Backus C., Mather J., Hauser M., Weiss R., Wilkinson D., Gulkis S., Boggess N., Cheng E., Kelsall T., Lubin P., Meyer S., Moseley H., Murdock T., Shafer R., Silverberg R., and Wright E. COBE Differential Microwave Radiometers: Instrument design and implementation. *Astrophys. J.*, 1990, v. 360, 685–695.
47. Smoot G.F., Bennett C.L., Kogut A., Wright E.L., Aymon J., Boggess N.W., Cheng E.S., de Amici G., Gulkis S., Hauser M.G., Hinshaw G., Jackson P.D., Janssen M., Kaita E., Kelsall T., Keegstra P., Lineweaver C., Loewenstein K., Lubin P., Mather J., Meyer S.S., Moseley S.H., Murdock T., Rokke L., Silverberg R.F., Tenorio L., Weiss R., and Wilkinson D.T. Structure in the COBE differential microwave radiometer first-year maps. *Astrophys. J. Letters*, 1992, v. 396(1), L1–L5.
48. Bennett C.L., Kogut A., Hinshaw G., Banday A.J., Wright E.L., Gorski K.M., Wilkinson D.T., Weiss R., Smoot G.F., Meyer S.S., Mather J.C., Lubin P., Loewenstein K., Lineweaver C., Keegstra P., Kaita E., Jackson P.D., and Cheng E.S. Cosmic temperature fluctuations from two years of COBE differential microwave radiometers observations. *Astrophys. J.*, 1994, v. 436, 423–442.
49. Bennett C.L., Banday A.J., Gorski K.M., Hinshaw G., Jackson P., Keegstra P., Kogut A., Smoot G.F., Wilkinson D.T., and Wright E.L. Four-Year COBE DMR Cosmic Microwave Background Observations: Maps and Basic Results. *Astrophys. J.*, 1996, v. 464, L1–L4 and plates L1–L3.
50. Hoyle F. A new model for the expanding universe. *Monthly Not. Roy. Astron. Soc.*, 1948, v. 108(5), 372–382.
51. Bondi H. and Gold T. The steady-state theory of the expanding universe. *Monthly Not. Roy. Astron. Soc.*, 1948, v. 108(3), 252–270.
52. Lemaitre G. Un univers homogène de masse constante et de rayon croissant, rendant compte de la vitesse radiale des nébuleuses extragalactiques. *Annales de la Société scientifique de Bruxelles*, 1927, v. 47, 49–59.
53. Guth A.H. Inflation and the new era of high precision cosmology. *MIT Physics Annual*, 2002, 28–39.
54. Smoot G.F. Our age of precision cosmology. *Proceedings of the 2002 International Symposium on Cosmology and Particle Astrophysics* (CosPA 02), X.G. He and K.W. Ng, Editors, World Scientific Publications, London, U.K., 2003, 314–326.
55. Danese L. and Partidge R.B. Atmospheric Emission Models: Confrontation between Observational Data and Predictions in the 2.5–300 GHz Frequency Range. *Astrophys. J.*, 1989, v. 342, 604–615.
56. Partridge R.B. 3 K: the Cosmic Microwave Background Radiation. Cambridge University Press, Cambridge, 1995, p. 103–160.
57. Lay O.P and Halverson N.W. The Impact of Atmospheric Fluctuations on Degree-Scale Imaging of the Cosmic Microwave Background. *Astrophys. J.*, 2000, v. 543, 787–798.
58. Planck M. The theory of heat radiation. P. Blakiston's Son & Co., Philadelphia, PA, 1914.
59. Robitaille P.-M.L. The solar photosphere: evidence for condensed matter. *Prog. in Phys.*, 2006, v. 2, 17–21.
60. Sabins F.F. Remote sensing: principles and applications. W. H. Freeman and Company, San Francisco, CA, 1978.
61. Lillesand T.M., Kiefer R.W., and Chipman J.W. Remote sensing and image interpretation (6th Edition). John Wiley and Sons, Hoboken, N.J., 2008.
62. Ulaby F.T., Moore R.K., and Fung A.K. Microwave remote sensing active and passive — Volume 2: Radar remote sensing and surface scattering and emission theory. London, Addison-Wesley Publishing Company, 1982, p. 880–884.

63. Maréchal Y. The hydrogen bond and the water molecule: the physics and chemistry of water, aqueous and bio-media. Elsevier, Amsterdam, 2007.
64. Dyke T.R. and Muenter J.S. Microwave spectrum and structure of hydrogen bonded water dimer. *J. Chem. Phys.*, 1974, v. 60, 2929–2930.
65. Dyke T.R., Mack K.M., and Muenter J.S. The structure of water dimer from molecular beam electric resonance spectroscopy. *J. Chem. Phys.*, 1977, v. 66, 498–510.
66. Smith J.D., Cappa C.D., Wilson K.R., Messer B.M., Cohen R.C., and Saykally R.J. Energetics of hydrogen bond network rearrangements in liquid water. *Science*, 2004, v. 306, 851–853.
67. Weiss R. Measurements of the cosmic background radiation. *Ann. Rev. Astron. Astrophys.*, 1980, v. 18, 489–535.
68. Matsumoto T., Hayakawa S., Matsuo H., Murakami H., Sato S., Lange A.E., and Richards P.L. The submillimeter spectrum of the cosmic background radiation. *Astrophys. J.*, 1988, v. 329, 567–571.
69. Woody D.P. An observation of the submillimeter cosmic background spectrum. University of California, Berkeley, 1975.
70. Singal J., Fixsen D.J., Kogut A., Levin S., Limon M., Lubin P., Mirel P., Seiffert M. Villela T., Wollack E. and Wuensche C.A. The ARCADE 2 instrument. arXiv: 0901.0546.
71. 71.Kogut A., Fixsen D.J., Levin S.M., Limon M., Lubin P.M., Mirel P., Seiffert M., Singal J., Villela T., Wollack E., and Wuensche C.A. ARCADE 2 observations of galactic radio emission. arXiv: 0901.0562.
72. Atkinson N. Cosmic radio noise booms six times louder than expected. Universe Today, January 7, 2000, http://www.universetoday.com/2009/01/07/cosmic-radio-noise-booms-six-times-louder-than-expected/
73. Mather J.C. Far infrared spectrometry of the Cosmic Background Radiation. University of California, 1974.
74. Wilkinson D. The microwave background anisotropies: observations. *PNAS*, 1998, v. 95(1), 29–34.
75. Harris L. The optical properties of metal blacks and carbon blacks. MIT and The Eppley Foundation for Research, Monograph Ser. 1, New Port, R.I., Dec. 1967.
76. Harris L., McGuiness R.T., and Siegel B.M. The preparation and optical properties of gold black. *J. Opt. Soc. Am.*, 1948, v. 38, 582.
77. Emerson and Cuming Microwave Products (Canton, MA). Technical Bulletin 2–6 (revised).
78. Emerson and Cuming Microwave Products. Technical Reference: ECCOSORB® CR Two-Part Castable Load Absorber Series. http://www.eccosorb.com/file/958/cr.pdf
79. Hemmati H., Mather J.C., and Eichhorn W.L. Submillimeter and millimeter wave characterization of absorbing materials. *Appl. Optics*, 1985, v. 24, 4489–4492.
80. Touloukian Y.S. and DeWitt D.P. Thermal radiative properties of nonmetallic solids. Vol. 8. In: *Thermophysical Properties of Matter*, IFI/Plenum, New York, N.Y., 1972.
81. Kraus J.D. Antennas. McGraw-Hill Book Company, New York, N.Y., 1988.
82. Balanis C. Modern antenna handbook. John Wiley and Sons, Inc., Hoboken, N.J., 2008.
83. Johnson R.C. Antenna engineering handbook. McGraw-Hill Company, New York, N.Y., 1993.
84. Shen Z. and Feng C. A new dual-polarized broadband horn antenna. *IEEE Ant. Wireless Prop. Lett.*, 2005, v. 4, 270–273.
85. Bruns C., Leuchtmann P., and Vahldieck R. Analysis and simulation of a 1–18 GHz broadband double-ridged horn antenna. *IEEE Trans. Electromagn. Comp.*, 2003, v. 45(1), 55–60.
86. PLANCK website, http://www.rssd.esa.int/index.php?project=PLANCK&page=index.
87. Bard S., Stein J., and Petrick S.W. Advanced radiative cooler with angled shields. Spacecraft radiative transfer and temperature control (T.E. Horton, Ed). *Prog. Astronautics & Aeronautics*, 1982, v. 83, 249–258.
88. Taylor J.R. An introduction to error analysis: the study of uncertainties in physical measurements. University Science Books, Mill Valley, CA, 1982.
89. Giorgi P.G. Influence of the angular response on Fourier absolute spectrometry the case of COBE-FIRAS. *Infrared Phys. Tech.*, 1995, v. 36, 749–753.
90. Battistelli E.S., Fulcoli V., and Macculi C. The CMBR spectrum: new upper limits for the distortion parameters y and μ. *New Astronomy*, 2000, v. 5, 77–90.
91. Salvatera R. and Burigana C. A joint study of early and late spectral distortions of the cosmic microwave background and of the millimetric foreground. *Mon. Not. Royal Astron. Soc.*, 2002, v. 336(2), 592–610.